Shell-mediated tunnelling between (anti-)de Sitter vacua

Stefano Ansoldi[*]

Center for Theoretical Physics, Laboratory for Nuclear Science and Department of Physics, Massachusetts Institute of Technology
and International Center for Relativistic Astrophysics (ICRA), Pescara, Italy[†]

Lorenzo Sindoni[‡]

International School for Advanced Studies, SISSA/ISAS via Beirut, 2-4— I-34014 Miramare, and
INFN, Sezione di Trieste, Trieste (TS), Italy

We give an extensive study of the tunnelling between arbitrary (anti-)de Sitter spacetimes separated by an infinitesimally thin relativistic shell in arbitrary spacetime dimensions. In particular, we find analytically an exact expression for the tunnelling amplitude. The detailed spacetime structures that can arise are discussed, together with an effective *regularization scheme* for *before tunnelling* configurations.

I. INTRODUCTION

The study of vacuum decay initiated more than 30 years ago with the work of Callan and Coleman [1,2]; in the following years the interest in the subject increased and the possible interplay of true vacuum bubbles with gravitation was also studied [3,4], together with bubbles collisions and their importance in the early universe [5,6]. At the same time, and as opposed with the true vacuum bubbles of Coleman *et al.*, false vacuum bubbles were also considered. In connection with gravity, the behavior of regions of false vacuum, first studied by Sato *et al.* [7–12], was, for example, analyzed in [13–20]. For additional papers analyzing it in the context of inflation, we refer the reader to [21–23]; interesting links with more phenomenologically oriented approaches can also be drawn, as witnessed, for instance, by the recent [24].

In these last works, a minisuperspace approximation was adopted to quantize the system. In more detail, since general relativistic shells[1] can be used as a convenient model and since in spherical symmetry the system has only one degree of freedom, standard semiclassical methods might be suitable to analyze the decay process (see [25] for an early, *in principle*, discussion of this point). In connection with cosmology, spaces *equipped* with a cosmological constant (i.e. de Sitter space and generalizations) have been naturally considered. In this context it is also worth remarking the important role that they play in connection with the problem of gravitational entropy,

causal structure, and the presence of horizons (see, for instance [26–30] as well as the suggestive [31]).

Notwithstanding many interesting results, after 30 years, and with different flavors, the problem of the stability of (the de Sitter) vacuum in connection with the dynamics of false vacuum bubbles, is still a debated one [19,32,33].

The still open issues are highly nontrivial and go back to the, also long-lasting, problem of formulating a consistent framework for a quantum theory of gravity [34–40], but we will not take explicitly this point of view here. We will instead analyze a specific situation, described below, in which the nucleation rate can be computed exactly in arbitrary spacetime dimensions. We will, then, explicitly compute in closed form the nucleation rate in the semiclassical approximation, compare it with existing results, and discuss in detail the associated spacetime structures: an analysis of how quantum effects may be relevant in the context of *tunnelling from nothing configurations* [41] will also be given. These results extend some results present in the literature (for instance [16,42–44]) and can also provide a useful limiting case of more general situations, for instance those discussed in [33]. At the same time, to consider spacetimes of higher dimensionality and negative cosmological constant is especially important in view of recent results in the context of the anti-de Sitter (AdS)/conformal field theory (CFT) correspondence [45] and of the braneworld cosmological scenario [46,47] (see also [48] and references therein for a study in the context of noncommutative branes).

Apart from the papers already cited above, the instanton approach has also been discussed by other authors (see for instance [49–51]) and although it will not be directly related to the present paper, we cannot avoid mentioning the suggestive relationship between the decay of the cosmological constant, membranes generated by higher rank gauge potentials and black holes, which have appeared in many papers in the literature [52–62].

---

[*]ansoldi@trieste.infn.it;
http://www-dft.ts.infn.it/~ansoldi
[†]Mailing address: Dipartimento di Matematica e Informatica, Università degli Studi di Udine, via delle Scienze 206, I-33100 Udine (UD), Italy; INFN, Sezione di Trieste, Trieste, Italy
[‡]sindoni@sissa.it

[1]In this paper we will use interchangeably the terms *shell*, *bubble*, and *brane*, which in different *epochs* have appeared in the literature to designate the system under consideration.

The structure of the paper is the following: in Sec. II we recall the formalism by which a general relativistic thin spherical brane/shell can be described; this also gives us the opportunity to fix conventions and notations and briefly describe the canonical approach to its semiclassical quantization (subsection II C); a convenient dimensionless formalism is also introduced (subsection II D). We then directly come (Sec. III) to the main result of this paper, which is the calculation of the tunnelling rate between the classical configurations of the system, in arbitrary spacetime dimensions; the results for the cases of 3, 4, and 5 spacetime dimensions are explicitly presented with dedicated plots of the values of the action as a function of the two dimensionless parameters of the model (subsection III C). The exact results for the tunnelling amplitude/probability calculated in Sec. III correspond to specific transitions which take place in spacetime and that will be discussed later on, in a dedicated appendix. We discuss, instead, in the main text (Sec. IV) a proposal to regularize some spacetime configurations which appear to be singular, relating this issue to the description of the brane energy-matter content. In the concluding Sec. V, the results of the paper are summarized; two appendices follow with the detailed description of the parameter space of the system (Appendix A) and of all the Penrose diagrams associated with different values of the parameters of the problem (Appendix B): they are crucial to fully grasp the physical system under consideration.

II. SHELL IN $N + 1$ DIMENSIONS

In this section we are going to briefly review some results about the dynamics of codimension one branes in an $(N + 1)$-dimensional spacetime, where, under the words *codimension one brane*, we understand an N-dimensional hypersurface Σ separating the $(N + 1)$-dimensional manifold in two domains, $\mathcal{M}_-$ and $\mathcal{M}_+$ having Σ as a common part of their boundary: in brief $\partial \mathcal{M}_- \cap \partial \mathcal{M}_+ = \Sigma$. In what follows we are going to use the clear notation of [63]: the formulation developed there can be readily extended to higher dimensions, just by letting the indices run on an extended set of values. We will thus quickly report this paraphrase with the purpose of recalling some notations and conventions. In particular let us choose two arbitrary systems of $N + 1$ independent vector fields $E_{\pm(a)}$ in $\mathcal{M}_\pm$, respectively, with dual forms $\Omega_\pm^{(b)}$. Denoting with $g_{(\pm)}$ the four dimensional metric tensors in the two manifolds we can write,[2] in general,

$$g_{(\pm)} = g_{(\pm)ab} \Omega_{(\pm)}^{(a)} \otimes \Omega_{(\pm)}^{(b)};$$

in our notation Latin indices a, b (as well as all other Latin indices) will vary in the set $\{0, 1, 2, \ldots, N\}$.

Let us first concentrate our attention on Σ: it is also a manifold, as $\mathcal{M}_\pm$, and we will denote by $e_{(\mu)}$ an N-dimensional system of (commuting) independent vector fields on Σ, with dual system $\omega^{(\nu)}$; the indices μ and ν (as well as all other Greek indices) will vary in the set $\{0, 1, \ldots, N - 1\}$. Because of the physical interpretation we will be interested in the case in which Σ is embedded as a *timelike* surface in $\mathcal{M}_+$. Since Σ is timelike the normal to Σ in $\mathcal{M}_\pm$ is a spacelike vector n, which we choose normalized so that $\langle n, n \rangle = +1$. Moreover, our convention is that the normal points from the "$-$" to the "$+$" domain of spacetime.

The components of n (an *unambiguously* defined *non-null* vector) will be different, in general, when measured by an observer in $\mathcal{M}_-$ or by one in $\mathcal{M}_+$, according to the following definition:

$$n_a|_\pm = \langle n, E_{(a)} \rangle|_\pm = \langle n, E_{\pm(a)} \rangle.$$

In terms of n the *extrinsic curvature* of the surface Σ can be expressed as[3]

$$K_{\mu\nu} = \langle n, \nabla_{e_{(\mu)}} e_{(\nu)} \rangle$$

and, in general, it is different on the $-$ and $+$ side. Moreover, by the Gauss-Codazzi formalism, the geometry of spacetime around Σ can be described in terms of the intrinsic geometry of the hypersurface and of its extrinsic curvature. In the spirit of this formalism, let us denote by h the intrinsic metric of the hypersurface Σ, i.e.

$$h = h_{\mu\nu} \omega^{(\mu)} \otimes \omega^{(\nu)}.$$

When we will work with quantities defined in the *bulk* we will need to distinguish the ones defined in $\mathcal{M}_+$ from the ones defined in $\mathcal{M}_-$, and to this end we will use, as we did above, "$\pm$" superscripts or subscripts. In many cases we will also be interested in the *jump* of these quantities across Σ: for instance, if we consider the extrinsic curvature, we may need to consider the difference $K_{\alpha\beta}^+ - K_{\alpha\beta}^-$: following [63,64] we are going to rewrite this difference as $[K_{\alpha\beta}]$. Throughout this paper this will be *the only meaning* that we will give to the square brackets, i.e.

$$[A] \stackrel{\text{def.}}{=} A^+ - A^-.$$

To avoid confusion no other use of the square brackets will be done.

A. Junction conditions

The brane Σ can be more than just a mathematical surface, i.e. we can (and, in most of the cases, we want

---

[2]In a few equations below, we will use the notation $\langle -, - \rangle$ to denote the scalar product. We also anticipate the notation $\nabla_Y X$ for the covariant derivative of the vector field X in the direction of the vector field Y.

[3]We stress the normalization condition on n.

to) equip it with a matter-energy content: it is then an infinitesimally[4] thin distribution of matter energy. Thanks to the above mentioned Gauss-Codazzi formalism, we can rewrite Einstein equations to make explicit the contribution from the localized matter. Then, the dynamics of Σ as a surface separating $\mathcal{M}_+$ from $\mathcal{M}_-$ is obtained solving the following system of equations,

$$K^+_{\alpha\beta} - K^-_{\alpha\beta} \equiv [K_{\alpha\beta}] = 8\pi G_{N+1}(S_{\alpha\beta} - h_{\alpha\beta}S/2); \quad (1)$$

these are Israel's junction conditions [63,64] which relate the jump in the extrinsic curvature $[K_{\mu\nu}]$, i.e. the "jump" in the way the surface is embedded in each geometry, to the stress-energy tensor $S_{\mu\nu}$ of the matter contained on Σ. The tensor S must also satisfy a conservation equation,

$$\langle^{(N)}\nabla, S\rangle_\mu = [T(n, e_{(\mu)})],$$

where T is the stress-energy tensor describing the content of the complete spacetime manifold. Once we have specified the matter content of the bulk (and hence the geometry according to Einstein equations) the description of the dynamics of the system is obtained by solving the system of equations (1); we refer the reader to [63,66] for additional material and related considerations.

B. Spherical symmetry

The setup that is of interest for us is a simplified one, in which all the system is spherically symmetric and the surface stress-energy tensor is that of the, so-called, *tension model*, with

$$S = -\kappa h,$$

where $\kappa > 0$ is a constant called the tension of the brane. In what follows, it will be convenient to also define

$$\tilde{\kappa} = 4\pi(N-2)G_{N+1}\kappa.$$

Thanks to the spherical symmetry, the *system* of equations (1) can then be reduced to a single equation [67],

$$R(\epsilon_- \sqrt{\dot{R}^2 + f_-(R)} - \epsilon_+ \sqrt{\dot{R}^2 + f_+(R)}) = \tilde{\kappa}R^2; \quad (2)$$

in the above, $f_\pm(r_\pm)$ are the metric functions of the static line element adapted to the spherical symmetry, i.e., taking the four dimensional case as a convenient example, we choose in both $\mathcal{M}_\pm$ the coordinate system $x^a_\pm = (t_\pm, \theta_\pm, \phi_\pm, r_\pm)$ corresponding to the basis vectors $e_{t_\pm}$, $e_{\theta_\pm}$, $e_{\phi_\pm}$, and $e_{r_\pm}$, such that the metric is reduced to the form $g_{(\pm)ab} = \text{diag}(-f_\pm(r_\pm), r^2_\pm, r^2_\pm \sin^2\theta_\pm, 1/f_\pm(r_\pm))$. Generalizations to spacetimes with higher dimensionality are just more cumbersome to write but trivial in their substance. In these coordinate systems, we denote the

radius of the brane by $R(\tau)$, where τ is the proper time of an observer comoving with the brane and an overdot denotes the derivative with respect to τ. Moreover, as anticipated in the introduction, we consider that this N-dimensional brane separates two $(N + 1)$-dimensional spacetimes of the de Sitter/anti-de Sitter type, in general with different cosmological constants $\Lambda_\pm$. We thus have

$$f_\pm(r_\pm) = 1 - \frac{2\Lambda_\pm}{N(N-1)}r^2_\pm.$$

Finally $\epsilon_\pm$ are signs, defined as

$$\epsilon_\pm(R) = \text{sign}(\langle n, e_{r_\pm}\rangle)|_{r_\pm=R}$$

and are crucial quantities to obtain the Penrose diagrams associated with the considered brane configuration.

C. The effective action/the momentum

Before proceeding with the analysis of the physical system that we introduced in the previous subsection, we believe it is useful to recall some important points about the structure of the junction conditions in spherical symmetry. For a generic junction between spherically symmetric spacetimes across a (spherical) brane carrying matter described by a given, but otherwise arbitrary, equation of state, it would prove very useful to extract an effective action for the dynamics of the brane starting directly from the Einstein-Hilbert action and from a suitable action for the matter fields and the brane [67]. This is the content of a consistent literature on the subject [68–76] among which we would like to single out the more general, and recent, [77]: the problem is not trivial at all, because of the same subtleties that appear, for instance, in the Hamiltonian formulation of general relativity. Among the various possible approaches we will closely follow the quantization procedure originally proposed by Farhi, Guth, and Guven [16], which has, lately, been followed also in [67,78]. For the Lagrangian approach to the classical dynamics we will instead follow the clear and more general exposition of [77]. We summarize here the relevant elements of these approaches referring the reader to the literature for additional details. In particular, the effective action for the shell can be obtained starting from the Einstein-Hilbert action with the Gibbons-Hawking boundary terms [16,77,79]. Using the Gauss-Codazzi formalism [80], it is readily seen that the Einstein-Hilbert action for a spherical codimension one brane (which in our case will separate two domains of (anti-)de Sitter spacetime) can be decomposed in nondynamical bulk contributions (indeed, we consider the geometry of the bulk spacetimes $\mathcal{M}_\pm$ fixed) and a dynamical *boundary* contribution described in terms of the extrinsic curvature of the brane Σ. It is enlightening (and, perhaps, necessary) not to use all the freedom in fixing the coordinate systems. As an exemplification we do not use the freedom given by the reparametrization invariance with respect to the proper time of the brane

---

[4]Strictly speaking Σ is a source defined in a distributional way: for additional material on this point, the reader is referred, for instance, to [65].

and we, thus, introduce a lapse function $\mathcal{N}(s)$, so that the brane induced metric can be written as $h_{\mu\nu}^{(\mathcal{N})} = \text{diag}(-\mathcal{N}(s)^2, R^2(s), \ldots)$ in the coordinates $(s, R, \ldots)$ (the "…" stand for the trivial spherically symmetric part). Then, following [67,77], the effective action for the degrees of freedom associated with the radial and time coordinates takes the form

$$S_{\text{eff}} \propto \int \left\{ R^{N-2} \left[\epsilon\sqrt{\dot{R}^2 + \mathcal{N}^2 f(R)} \right. \right.$$
$$\left. - \dot{R} \operatorname{arctanh}\left(\frac{\dot{R}}{\epsilon\sqrt{\dot{R}^2 + \mathcal{N}^2 f(R)}}\right)^{\operatorname{sign}(f)} \right]$$
$$\left. - \tilde{\kappa}\mathcal{N}R^{N-1} \right\} d\tau. \quad (3)$$

Thus, the effective Lagrangian of the system is given by

$$\mathcal{L} = P^{(\mathcal{N})}\dot{R} - \mathcal{H},$$

where, following [67], we have defined the effective Hamiltonian as

$$\mathcal{H} = -R^{N-2}[\epsilon\sqrt{\dot{R}^2 + \mathcal{N}^2 f(R)}] + \tilde{\kappa}\mathcal{N}R^{N-1}$$

and the effective momentum as

$$P^{(\mathcal{N})}(R, \dot{R}) = -R^{N-2}\left[\operatorname{arctanh}\left(\frac{\dot{R}}{\epsilon\sqrt{\dot{R}^2 + \mathcal{N}^2 f(R)}}\right)^{\operatorname{sign}(f)} \right]. \quad (4)$$

Then, the equations of motion for the R and $\mathcal{N}$ degrees of freedom are

$$\frac{d\mathcal{H}}{d\tau} = \frac{\dot{\mathcal{N}}}{\mathcal{N}}\mathcal{H} \quad \text{and} \quad \mathcal{H}(R, \dot{R}, \mathcal{N}) = 0;$$

the second equation is a first integral of the former one, and is the *Hamiltonian constraint*. We see that it encodes all the information about the dynamics of the system, being identical to the only remaining junction condition. The first equation is the second order equation of motion of the system, given by the total derivative with respect to the proper time of the Hamiltonian constraint. In what follows, we will be mostly interested in the expression of the momentum evaluated on a solution of the equation of motion. In order to build a canonical structure (as it is done, for example, in [46]) we first have to prove the existence of a well-defined symplectic structure on the phase space of the Lagrangian system; in particular, the Legendre transform has to be invertible, which in our case means nothing but the invertibility of the conjugate momentum as a function of the velocity [81]. As appreciated already in [16], for generic codimension one branes this cannot be proved to be always satisfied.[5] However, for the

system under consideration the canonical structure always exists and $P^{(\mathcal{N})}$ can rigorously be considered the canonical momentum conjugate to the coordinate R; thus, in the specific case of interest here, the canonical construction of the corresponding quantum theory is a well posed problem. To prove this statement, let us consider

$$\frac{\partial P^{(\mathcal{N})}}{\partial \dot{R}} = -R^{N-2}\left[\frac{1}{\epsilon\sqrt{\dot{R}^2 + \mathcal{N}^2 f(R)}} \right].$$

This quantity can be zero if and only if two conditions are simultaneously satisfied:

(1) $\epsilon_+ = \epsilon_-$;
(2) there is a point R in the configuration space such that $f_+(R) = f_-(R)$.

For our particular choice of branes in (anti-)de Sitter spacetime, we see that in order for the second condition to hold we must have $\Lambda_- = \Lambda_+$; but this implies[6] $\epsilon_+ = -1$, $\epsilon_- = +1$ so that the first condition then fails. Thus, for the class of junctions that we are considering one can always build a canonical structure.

D. Dimensionless formalism

Following, for instance, [82], it is possible to determine the classical dynamics of the system by studying an equivalent one dimensional problem for the radial degree of freedom R, taking also into account the values of the signs $\epsilon_\pm(R)$.

Before proceeding we will set up a different system of dimensionless quantities, in order to remove the arbitrariness in the definition of the normalization of the cosmological constants and of the bubble's tension. If we define the quantities

$$x = \tilde{\kappa}R, \qquad \bar{\tau} = \tilde{\kappa}\tau, \qquad \lambda_\pm = \frac{2\Lambda_\pm}{\tilde{\kappa}^2 N(N-1)},$$
$$\alpha = \lambda_- + \lambda_+, \qquad \beta = \lambda_- - \lambda_+,$$

Eq. (2) then becomes[7]

$$-[\epsilon\sqrt{\dot{x}^2 + 1 - \lambda x^2}]x = x^2. \quad (5)$$

For completeness we also report the dimensionless form of the effective momentum (4) when we impose the gauge choice $\mathcal{N} \equiv 1$:

$$\bar{P}(x, \dot{x}) = -x^{N-2}\left[\epsilon \operatorname{arctanh}\left(\frac{\dot{x}}{\sqrt{\dot{x}^2 + f(x)}}\right)^{f/|f|} \right]. \quad (6)$$

This quantity will be central in what follows, but for the moment we keep our attention on Eq. (5). Despite its unusual look, it is easily proved that it is equivalent to a system of equations, which, in the notation that we are

---

[5] In these cases the quantum theory cannot be built with the canonical formalism. Alternative formulations using the path-integral approach have been considered in the seminal work of Farhi, Guth, and Guven [16].

[6] This can be easily seen from the junction condition (2) remembering that $\tilde{\kappa} > 0$.

[7] An overdot will denote, from now on, a derivative with respect to $\bar{\tau}$.

using, takes the form

$$\begin{cases} \dot{x}^2 + \bar{V}(x) = 0 \\ \epsilon_\pm(x) = -\text{sgn}(\beta \pm 1) \end{cases}, \qquad (7)$$

where the potential $\bar{V}(x)$ has a simple parabolic form

$$\bar{V}(x) = 1 - \frac{x^2}{x_0^2} \qquad (8)$$

and x_0, the turning point, is given by

$$x_0^2 = \frac{4}{1 + 2\alpha + \beta^2}, \qquad (9)$$

when the right-hand side is positive; otherwise there are no nontrivial classical solutions. All the solutions of the problem can be easily classified according to the values of α and β: we refer the reader to Appendix A for details. The expressions for the signs $\epsilon_\pm$ relate, instead, the global geometrical structure of spacetime for this brane configuration only to the difference between the inner and outer cosmological constants, not to the details of the trajectory itself. This is a portion of the content of the junction condition, that is necessary for the description of the global spacetime structure: a careful discussion of this point can be found in Appendix B.

The form of (5) for a brane separating two (anti-)de Sitter spacetimes, which, in turn, is responsible for the simple quadratic form of the potential (8), allows an exact solution of this particular case. It is, in fact, not difficult to see that (5) has:

(1) the *trivial solution* $x(\bar{\tau}) \equiv 0$, which always exists;
(2) the solution

$$x(\bar{\tau}) = x_0 \cosh\left(\frac{\bar{\tau} - \bar{\tau}^{(0)}}{x_0}\right), \qquad (10)$$

which satisfies the initial condition $x(\bar{\tau}^{(0)}) = x_0$; this solution is known as the *bounce solution* and exists only if the condition

$$1 + 2\alpha + \beta^2 > 0$$

is satisfied.

We also, incidentally, note that

$$\beta = \pm 1 \Leftrightarrow \frac{1}{x_0^2} = \lambda_\mp,$$

i.e. when $|\beta| = 1$ the turning point radius coincides with one of the two cosmological horizons, if they exist. We also anticipate that a more careful analysis of the trivial solution $x(\bar{\tau}) \equiv 0$ will be required, since, although it is given to us by the mathematics of the problem, we are mostly interested in its physical role, especially when we will turn on (semiclassical) quantum effects (see Sec. IV).

III. TUNNELLING

Using the notation introduced in the last section we can now describe how the semiclassical regime of the brane dynamics looks. In particular we can consider the tunnelling between the zero-radius solution towards the bouncing solution (10), and vice versa.

For example in one direction the semiclassical picture is as follows: we have a brane, of very small radius; of course, when it is very small, the quantum properties of its matter content will be non-negligible (we will further discuss this issue later on in Sec. IV) and their interplay with gravity will be nontrivial; although we do not know the full quantum gravity description of the system, we will consider that, thanks to quantum effects, the brane will have a certain probability to tunnel under the potential barrier given by the effective potential (8) into the bounce solution. When emerging after the tunnelling quantum effects will likely become less and less important as compared with gravitational ones (and as far as the interaction with the bulk spacetime is concerned), so that the evolution of the brane will closely resemble that of the classical junction. This is not the case in the first stage of the evolution, involving the tunnelling process, and we will try to understand, at least at an effective level, the "responsibilities" of both the quantum and gravitational realms in this process. In particular, quantum effects will be considered in a modification at small scales of the stress-energy tensor (see Sec. IV). Gravitational effects, at small scales, are also present, and described by the geometric character of Israel junction conditions. We think that our description might be able to take into account both these effects, at least within the limits represented by the semiclassical approximation. In this sense, although our treatment will be effective, it will give us the possibility to consistently solve the ambiguity arising at the mathematical level and represented by the $x(\bar{\tau}) \equiv 0$ solution. We will suggest that, at the semiclassical level, a more detailed treatment of both, the quantum and gravitational aspects, is unlikely to be necessary.

A. Tunnelling trajectories

For the system under consideration, a tunnelling trajectory can be described by constructing the instanton in the Euclidean sector. The construction of the instanton in the general case is still an unsolved problem: we will follow the approach of [16]; moreover, the problems left open in [16] do not affect the present case. In fact it is easy to see that in our case the instanton describing the tunnelling can always be constructed without the necessity to introduce the *pseudomanifold* that in [16] was necessary to deal with multiple covering of points in the Euclidean sector. Moreover the different descriptions of the tunnelling process that were obtained in [16] using the canonical or the path-integral approaches in our case also coincide, because they are consequences of properties of the dynamical

variables during the tunnelling trajectory which are not present in the system that we are considering (please, see [83–85] for a more detailed description of these issues).

In this way we know that the tunnelling can be described directly at the effective level, where, the relevant aspects of the Euclidean junction can be determined by the Wick rotated classical effective system. We thus define $\bar{\tau}_e = -i\bar{\tau}$; then, denoting with a prime the derivative with respect to $\bar{\tau}_e$, we have that the Euclidean system is obtained with the formal substitutions $\dot{x} \rightarrow ix'$ for the "velocity" and

$$\bar{P} \rightarrow i\bar{P}_e$$

for the momentum (it is not difficult to prove that the above *substitution rules* are rigorous results and that they can be obtained performing a *Euclidean junction*, as done, for instance, in [16]). In particular

$$\bar{P}_e(x, x') = -x^{N-2}\left[\arctan\left(\frac{x'}{\epsilon\sqrt{f(x) - (x')^2}}\right)\right]. \quad (11)$$

In this way, the tunnelling process can be modeled using the effective tunnelling trajectory, which solves the Euclidean equation:

$$-(x')^2 + 1 - (x/x_0)^2 = 0. \quad (12)$$

The analytic expression of the tunnelling trajectory of a brane expanding from zero radius at Euclidean time $\bar{\tau}_e = 0$ to the bouncing solution is

$$x(\bar{\tau}_e) = x_0 \sin(\bar{\tau}_e/x_0).$$

The opposite process is then described by

$$x(\bar{\tau}_e) = x_0 \cos(\bar{\tau}_e/x_0),$$

if we assume that at Euclidean time $\bar{\tau}_e = 0$ the brane starts contracting from x_0. These two processes occur with certain probabilities, whose amplitudes $\mathcal{A}$ can be expressed in the usual semiclassical approximation as

$$\mathcal{A}(0 \rightarrow x_0) \propto \exp(-I_e[x]),$$

where $I_e[x]$ is the Euclidean action and can be obtained as the integral of the Euclidean momentum evaluated on a solution of the Euclidean equation of motion (12). If, for simplicity, we define

$$I_e[x] = \frac{\Omega_{N-1}}{16\pi G_{N+1}} \frac{1}{\kappa^{N-1}} \bar{I}_e[x],$$

where Ω_{N-1} is the volume of $\mathbb{S}^{N-1}$, then $\bar{I}_e[x]$ can be obtained as

$$\bar{I}_e[x] = \int_0^{x_0} \bar{P}_e(x)dx. \quad (13)$$

We stress again that $\bar{P}_e(x)$ is the Euclidean momentum evaluated on a solution of the Euclidean equation of motion and can be obtained by substituting $x' = \sqrt{\bar{V}(x)}$ in

(11). We thus have

$$\bar{P}_e(x) = -x^{N-2}\left[\arctan\left(\frac{2\sqrt{\bar{V}(x)}}{(\beta + \omega)x}\right)\right],$$

where, to make writing more compact,[8] we have introduced the quantities $\omega_{\pm}$ defined as $\omega_{\pm} = \pm 1$.

Note that in the Euclidean case we have some freedom in appropriately choosing one of the possible branches of the inverse tangent function. Different choices will affect, in general, the result that we obtain for the action. As in [16] we observe that noncareful choices will make the action a discontinuous function of the parameters; this can be seen without difficulties. Preliminarily, let us anticipate that with the symbol "arctan," we will indicate the branch of the inverse tangent function with range in $[-\pi/2, \pi/2]$. Let us then consider $\beta \neq \omega$ and let us integrate by parts the integral (13). We obtain

$$\bar{I}_e[x] = -\left[\frac{x^{N-1}}{N-1}\arctan\left(\frac{2\sqrt{\bar{V}(x)}}{(\beta + \omega)x}\right)\right]\Big|_0^{x_0}$$

$$+ \left[\int_0^{x_0} \frac{x^{N-1}}{N-1} d\left(\arctan\left(\frac{2\sqrt{\bar{V}(x)}}{(\beta + \omega)x}\right)\right)\right].$$

Let us now consider the first term above. Clearly, if we chose the branch of the arctan function to be the one with range in $[-\pi/2, \pi/2]$, then we have

$$\lim_{\beta \rightarrow -\omega^-}\left[\frac{x^{N-1}}{N-1}\arctan\left(\frac{2\sqrt{\bar{V}(x)}}{(\beta + \omega)x}\right)\right]\Big|_0^{x_0} = -\frac{\omega\pi x_0^{N-1}}{2(N-1)}$$

but

$$\lim_{\beta \rightarrow -\omega^+}\left[\frac{x^{N-1}}{N-1}\arctan\left(\frac{2\sqrt{\bar{V}(x)}}{(\beta + \omega)x}\right)\right]\Big|_0^{x_0} = +\frac{\omega\pi x_0^{N-1}}{2(N-1)},$$

so that the action develops a discontinuity at $\beta = -\omega$. This discontinuity can be eliminated if we choose different branches of the inverse tangent functions (please remember that in the expression that we are considering we are using a compact notation to indicate the difference of two inverse tangent functions); in particular, the two discontinuities at $\beta = \pm 1$ can be eliminated by choosing:

(1) the branch with range $[-\pi, 0]$ for the arctan function containing quantities of the "+" spacetime;
(2) the branch with range $[-\pi, 0]$ for the arctan function containing quantities of the "−" spacetime.

Since in our notation "arctan" has range $[-\pi/2, \pi/2]$, this means that the equations above must be rewritten with the substitutions (Θ is the step function)

$$\arctan("+") \rightarrow \arctan("+") - \pi\Theta(\beta + 1)$$

---

[8]In view of the definition of the ω's, and of the meaning of the square brackets, the equation above is a shorthand for $\bar{P}_e(x) = -x^{N-2}(\epsilon_+ \arctan(\frac{2\sqrt{\bar{V}(x)}}{(\beta+1)x}) - \epsilon_- \arctan(\frac{2\sqrt{\bar{V}(x)}}{(\beta-1)x}))$.

and

$$\arctan(\text{“} - \text{”}) \rightarrow \arctan(\text{“} - \text{”}) - \pi\Theta(\beta - 1);$$

for the *jump* of the quantity which appears inside the expression of the Euclidean momentum, this implies the following substitution:

$$[\arctan] \rightarrow [\arctan] - \pi\Theta(1 - \beta^2).$$

In this way the action integral is continuous also at the points $\beta = -\omega$ and is given by the integral

$$\bar{I}_e[x] = -\int_0^{x_0} dx\, x^{N-2} \times \left(\left[\arctan\left(\frac{2\sqrt{\bar{V}(x)}}{(\beta + \omega)x}\right)\right] - \pi\Theta(1 - \beta^2)\right). \tag{14}$$

After these preliminary considerations, we can proceed to evaluate the tunnelling amplitude in the WKB approximation; as we anticipated and as we will see, in arbitrary spacetime dimensions this result can be expressed analytically in terms of known functions.

B. General result for the tunnelling amplitude

To calculate the first contribution to the integral (14) we proceed as follows. As a preliminary step, we observe that it can be written as a difference of two integrals with the same general structure. Let us then consider the two integrals containing the inverse tangent functions: small differences, which do not substantially affect the calculation, can be taken into account by properly using the ω's introduced above, as we already did in the expressions for the momentum. This said, we can perform[9] an integration by parts in (14). The terms evaluated at the limits of integration, which appear in this process, do vanish and by changing the integration variable from x to $\zeta = (x/x_0)^2$ (which also transforms the integration domain into the unit interval $(0, 1)$) we obtain the following expression:

$$\bar{I}_e[x] = -\frac{x_0^N}{4(N-1)} \times \left[(\beta + \omega)\int_0^1 \frac{\zeta^{(N-2)/2}}{\sqrt{1-\zeta}}\right. \\ \left. \times \frac{1}{1 - z_\omega\zeta}d\zeta\right] + \frac{\pi x_0^{N-1}}{(N-1)}\Theta(1 - \beta^2), \tag{15}$$

where

$$z_\omega = \left(1 - x_0\frac{\beta + \omega}{2}\right)\left(1 + x_0\frac{\beta + \omega}{2}\right). \tag{16}$$

When $z_\omega < 1$ one of the above integrals diverges since there is a pole of the integrand on the domain of integration. On the other hand, it is easy to see that the condition

[9]Strictly speaking this can be done only when $\beta \neq -\omega$. The cases in which $\beta = -\omega$ are trivial and can be dealt separately; or, more simply, since we already know from the discussion in the previous subsection that the action is continuous, we can just extend it to $\beta = -\omega$ by continuity.

$z_\omega < 1$ implies

$$\frac{x_0^2}{4}(\beta + \omega)^2 < 0$$

and cannot be realized for any choice of the parameters if a tunnelling trajectory has to exist. The value $z_\omega = 1$ can instead be obtained if $\beta = -\omega$ and we know that the action can be extended by continuity to these values, although the above procedure to calculate the integral is not valid. Thus, under the conditions $\beta \neq -\omega$, we have that $z_\omega > 1$ is satisfied and Eq. (15) gives

$$\bar{I}_e[x] = -\frac{x_0^N}{4(N-1)}\frac{\Gamma(N/2)\Gamma(1/2)}{\Gamma((N+1)/2)} \\ \times \left[(\beta + \omega)_2F_1\left(1, \frac{N}{2}, \frac{N+1}{2}, z_\omega\right)\right] \\ + \frac{\pi x_0^{N-1}}{(N-1)}\Theta(1 - \beta^2), \tag{17}$$

where Γ is the Euler's gamma function, $_2F_1$ the hypergeometric function. Note that x_0 depends on α, β and so the first factor of the formula, depending on the number of spacetime dimensions, cannot be ignored even for a qualitative description of the tunnelling amplitude.

C. Some cases of interest

It is useful to specialize the result (17) to particular situations. We are going to do this by considering the cases in which spacetime is three, four, and five dimensional. Below we are going to explicitly discuss these three cases. A comparative presentation of the results can be found in the contour plots of Fig. 1.

We start then with the three dimensional case, which is lower dimensional gravity; in three spacetime dimensions it seems more clear how to build a quantum theory out of the classical junction conditions [46]. Moreover three dimensional gravity is an interesting system by itself, it allows an easier visualization of some results and can be used for interesting specific toy models. Anyway, in this case we have $N = 2$ and we can express $_2F_1(1, 1; 3/2; x)$ in terms of elementary functions as

$$_2F_1\left(1, 1; \frac{3}{2}; y\right) = \frac{\arcsin(\sqrt{y})}{\sqrt{1-y}\sqrt{y}}. \tag{18}$$

Correspondingly the action becomes

$$\bar{I}_e = -\frac{x_0^2}{4}\frac{\Gamma(1)\Gamma(1/2)}{\Gamma(3/2)} \times \left[(\beta + \omega)\frac{\arcsin(\sqrt{z_\omega})}{\sqrt{1-z_\omega}\sqrt{z_\omega}}\right] \\ + \pi x_0\Theta(1 - \beta^2). \tag{19}$$

The corresponding probability is plotted as a function of β in Fig. 2 for some non-negative values of α and in Fig. 3 for some negative values of α.

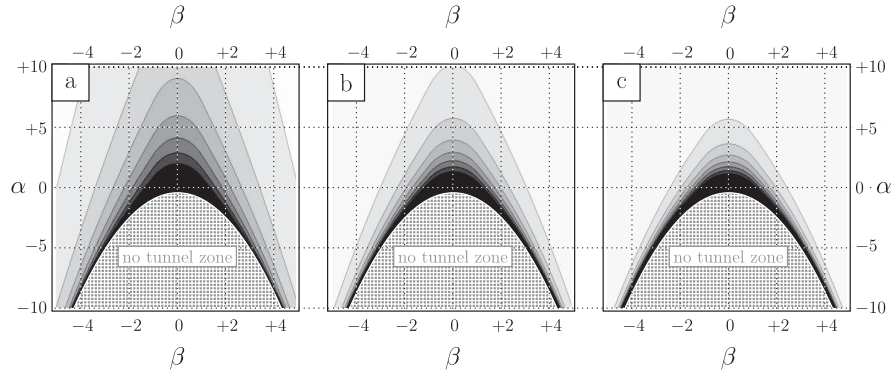Not many comments are necessary, of course, for the four dimensional case, the original arena on which this

FIG. 1. Contour plots of the values of the *tunnelling probability* in 3 (case a), 4 (case b), and 5 (case c) spacetime dimensions in the β-α plane. The area inside the crosshatched parabola in the bottom of each picture is the region in parameter space where tunnelling cannot occur since no bounce solutions exist (no tunnel zone). A better understanding of what happens close to the limiting parabola can be understood from the following Figs. 3, 5, and 7. Next to next contours indicate a jump of the probability of 0.1, with the lightest gray tone indicating the range (0.9, 1.0) and the darkest the range (0.0, 0.1). The same color indicates the same range of values of the probability in all the three subdiagrams.

calculation was performed. Again we can take advantage of a simple expression for the corresponding hypergeometric function

$$_2F_1(1, 3/2; 2; y) = \frac{2}{y\sqrt{1-y}} - \frac{2}{y}, \qquad (20)$$

which brings the final result in the form

$$\bar{I}_e = -\frac{\pi x_0^2}{4} \times \left(\left[\mathrm{sgn}(\beta + \omega) \frac{1 - (1 - z_\omega)^{1/2}}{z_\omega} \right] - \Theta(1 - \beta^2) \right). \qquad (21)$$

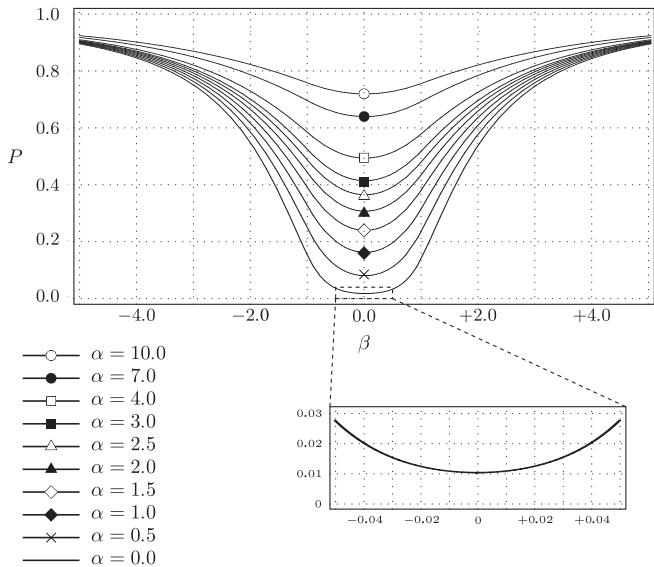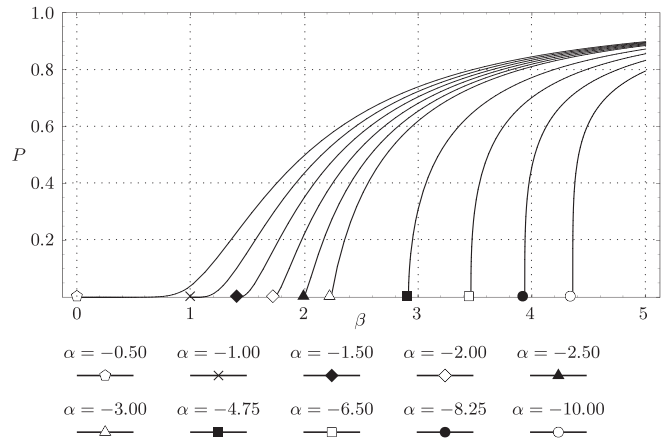

FIG. 2. Plots of the values of the *tunnelling probability* in a spacetime of dimension 3, as a function of β for fixed nonnegative values of α as listed above. The detailed behavior for $\alpha = 0$ around $\beta = 0$, is also shown (to better see that the probability is small but nonzero).

The plots of the probability as a function of β can be found in Fig. 4 for some non-negative values of α and in Fig. 5 for some negative values of α. This result is the same as the one obtained in [86] and it also reduces to the one calculated in [3]: it, thus, represents a useful consistency check.

Finally, the five dimensional case is interesting in the context of the Randall-Sundrum scenario. In this case, using

$$_2F_1\left(1, 2; \frac{5}{2}; y\right) = \frac{3}{2y}\left(\frac{\arcsin(\sqrt{y})}{\sqrt{1 - y}y^{1/2}} - 1\right), \qquad (22)$$

the result for the action integral can be put in the following form:

FIG. 3. Plots of the values of the *tunnelling probability* in a spacetime of dimension 3, as a function of β for fixed negative values of α as listed above. For $\alpha < -1/2$, not all values of β are allowed. We have put the mark on each curve in correspondence of the minimum value of β for which (at the given value of α) the tunnelling process can exist. For smaller values, the infinitely expanding solution, in fact, is not present.
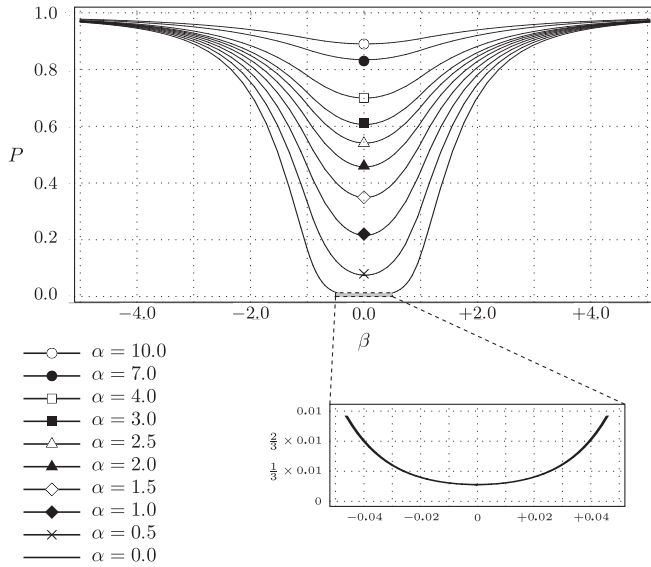
FIG. 4. Plots of the values of the *tunnelling probability* in a spacetime of dimension 4, as a function of β for fixed non-negative values of α as listed above. Again the detailed behavior for $\alpha = 0$ around $\beta = 0$ is shown (to better see that the probability, although very small, is nonvanishing).
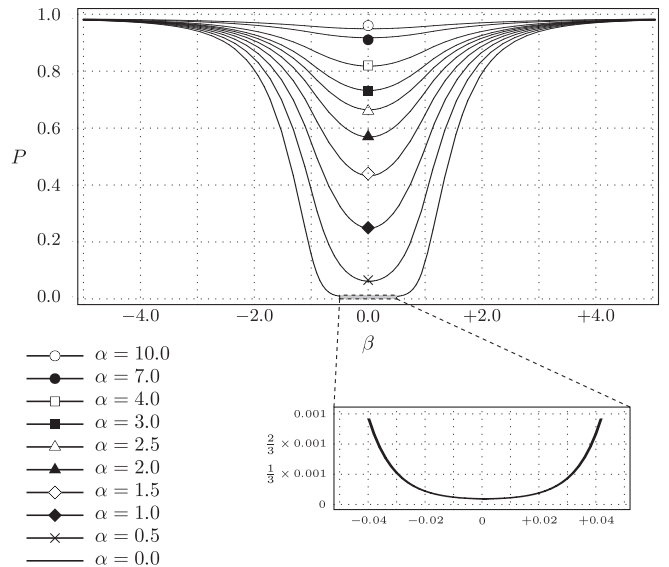
$$\bar{I}_e = -\frac{x_0^4}{12}\frac{\Gamma(2)\Gamma(1/2)}{\Gamma(5/2)}$$
$$\times\left[(\beta+\omega)\left(\frac{\arcsin(\sqrt{z_\omega})}{\sqrt{1-z_\omega}(z_\omega)^{3/2}}-\frac{1}{z_\omega}\right)\right]$$
$$+\frac{\pi x_0^3}{3}\Theta(1-\beta^2). \tag{23}$$

Again we present two plots of the corresponding probability as a function of β; Fig. 6 shows the behavior for some non-negative values of α, whereas plots for some negative values of α can be found in Fig. 7.
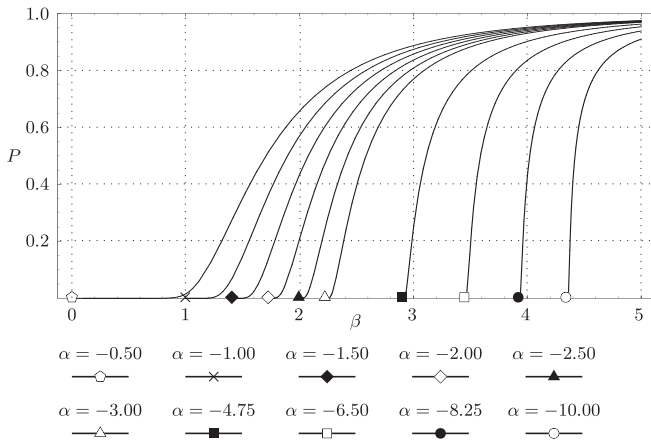

FIG. 5. Plots of the values of the *tunnelling probability* in a spacetime of dimension 4, as a function of β for fixed negative values of α as listed above. The same observations as in the case of 3 spacetime dimensions apply.
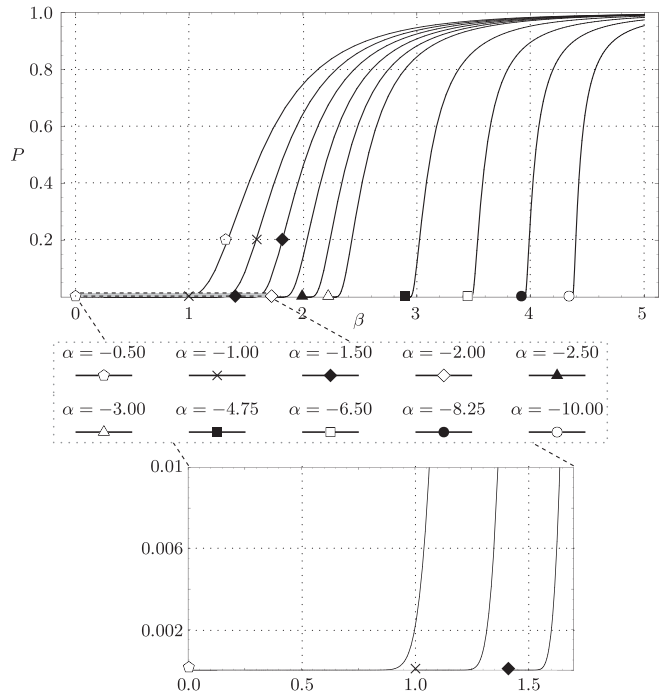

FIG. 6. Plots of the values of the *tunnelling probability* in a spacetime of dimension 5, as a function of β for fixed non-negative values of α as listed above. Again the detailed behavior for $\alpha = 0$ around $\beta = 0$ is shown (to better see that the probability, although much smaller than in the previous cases, is still nonvanishing).

FIG. 7. Plots of the values of the *tunnelling probability* in a spacetime of dimension 5, as a function of β for fixed negative values of α as listed above. For $\alpha < -1/2$, not all values of β are allowed. We have put the mark on each curve in correspondence of the minimum value of β for which (at the given value of α) the tunnelling process can exist and, the zoomed diagram, helps resolving the apparent superposition that arises between the curves obtained for $\alpha = -0.50, -1.00, -1.50$.

IV. DISCUSSION

Up to this point we have discussed the physics of the system rather quickly, focusing mainly on the mathematics necessary to describe the classical and the semiclassical phases. There is still a point which deserves a detailed discussion, since it involves nontrivial aspects of the dynamics of the brane. Indeed, the physical process we have considered is the tunnelling of spacetime, from a classical situation *representing* a spacetime containing a small brane to another classical configuration *describing* a bouncing brane. In our picture, the pretunnelling state is represented by the $x \equiv 0$ solution of the junction condition. Although this case might appear rather simple at first sight and one could be tempted to just state that the initial state is, for example, the full $\mathcal{M}_+$ spacetime (a point of view which has been taken, for example, in [67]), much more care has to be taken. The main reason is that when $x = 0$, the brane's world volume degenerates to a curve. Thus, the formalism that we used to describe the brane breaks down and the analysis that we have made cannot be considered as rigorous as it is in the case of the bouncing solutions. As a manifestation of this fundamental problem, we observe that the equations determining the $\epsilon_{\pm}$ signs do not hold for the particular solution $x \equiv 0$. In particular, for this solution the junction condition as written in (5) does not provide any mean to solve this problem.

A way out of this situation appears when we reflect on the fact that this process, although described semiclassically, is quantum in its true nature. Thus an approximation of the system which considers it completely classical *before the tunnelling*, i.e. in the degenerate configuration, might be too rough and might require a more careful consideration. During the tunnelling trajectory, and even more for the $x \equiv 0$ classical solution, quantum effects are supposed to be, if not dominant, at least relevant enough to modify the classical picture of the junction.

We will propose here an attempt to address the problem. Our proposal should be considered a first step further, but far from a first principle solution of the complex quantum problem; it just aims to show that the mathematical and physical aspects of the problem stated above can be dealt with by giving an effective formulation for the phenomena that might arise at small scales. At the same time, although we will just build an effective model, we will not be very demanding about its main properties: in this way, hopefully, the model, although effective, could mimic well enough effects produced by quantum gravity whatever will be their, still undiscovered, true nature.

In this respect, we would also like to point out the following: (i) the main effect of our proposal is to *slightly perturb* the effective potential (8) in the tunnelling region; then, we will (ii) show that the perturbed problem is free from ambiguities, and (iii) use for the *unperturbed case* the results obtained in the *perturbed one*, when the perturbation becomes smaller and smaller. To have a definite model, we will regard the small scale behavior of the matter composing the brane/shell as the physical origin for the perturbations (see below). On the other hand, the consequence of these perturbations in the effective formulation is completely *generic*: it is, in fact, possible to show that other physical motivations, as for instance the quantum properties of spacetime at small scales, could be reflected in a similar way in the effective formulation. For these reasons, we can regard our conclusions *model independent* to a high degree, at least within the context defined by the semiclassical approximation.

To introduce our model we can naturally think the brane as sourced by some matter fields whose nature is, ultimately, quantum. We thus argue that, although at large scales the approximation for the brane stress-energy tensor that we made in subsection II B might be rough but still appropriate, at small scales it will instead break down due to quantum effects. We will model these additional quantum effects by adding a term to the brane stress-energy tensor as follows:

$$S \longrightarrow S + S_q, \tag{24}$$

where the "quantum" contribution S_q will be parametrized as

$$S_q = \rho_q \boldsymbol{u} \otimes \boldsymbol{u} + \sigma_q \boldsymbol{h}. \tag{25}$$

The conservation equation for S_q under the assumption of spherical symmetry gives (we are going to use, from now on, the dimensionless versions of the parameters ρ_q and σ_q, which following the notation above, are called $\bar{\rho}_q$ and $\bar{\sigma}_q$)

$$\frac{d\bar{\rho}_q}{dx} + N\frac{\bar{\rho}_q}{x} = \frac{d\bar{\sigma}_q}{dx}. \tag{26}$$

We will choose preliminarily

$$\bar{\rho}_q(x) = ax^q \tag{27}$$

so that

$$\bar{\sigma}_q(x) = a\frac{q + N}{q}x^q. \tag{28}$$

In this case the junction condition becomes[10]

$$-[\epsilon_{(q)}\sqrt{\dot{x}^2 + 1 - \lambda x^2}]x = x^2\mu(x), \tag{29}$$

with

$$\mu(x) = 1 + \bar{a}x^q \tag{30}$$

---

[10]We remember that we are following the convention in which square brackets indicate the jump of the enclosed quantity, i.e. the difference of it when evaluated in the '+' and '−' domains. We are now using the suffix "…q" or "…(q)" to indicate quantities when the energy momentum tensor is modified, as described in the text, to take into account quantum effects; thus the two signs will now be $\epsilon_{(q)\pm}$.

and, for short, $\bar{a} = a(q + N)/q$. Now we are going to slightly restrict the parameters $\bar{a}$ and q to make these general settings appropriate for our model. In particular, the modification to the stress-energy tensor, described by $\bar{a}$ and q was introduced to model the quantum effects at small scales; thus it should be negligible at large scales and this can be achieved if $q + 1 < 0$, i.e. $q < -1$.

We can now compute the modified effective potential $\bar{V}_q$. The potential turns out to be

$$\bar{V}_q(x) = -\frac{x^2[\beta^2 + 2\alpha(1 + \bar{a}x^q)^2 + (1 + \bar{a}x^q)^4]}{4(1 + \bar{a}x^q)^2} \quad (31)$$

$$\overset{x \to 0}{\leadsto} -\frac{\bar{a}^2}{4x^{-2q-2}} \quad (32)$$

$$\overset{\bar{a} \to 0}{\leadsto} \bar{V}(x) + \frac{(1 - \beta^2)\bar{a}^2}{2x^{-q-2}}. \quad (33)$$

Extracting the behavior of (31) for small x we get (32), whereas for small $\bar{a}$ the leading contribution is given by (33). These are useful results. Indeed we see from (32) that, quite generally, and certainly under the above $q < -1$ condition, the potential satisfies

$$\lim_{x \to 0^+} \bar{V}_q(x) = -\infty.$$

This implies that the $\bar{V}_q(x)$ allows not only the bounce brane junction, as $\bar{V}(x)$ does, but also bounded solutions. Thus the addition of the S_q term to the stress-energy tensor, which in our picture is supposed to take into account quantum effects at small scales, in fact does his job by trading the $x \equiv 0$ solution for a bounded one of finite (i.e. nonvanishing) size. Moreover this solution exists under very general assumptions about the form of S_q, so that we do not have to commit ourselves too much about the underlying quantum gravity physics of which S_q is roughly supposed to take into account some effective semiclassical description. Looking now at Eq. (33) we also see that for small $\bar{a}$, apart from the evident qualitative difference at small scales, the potential resembles closely the nonperturbed one (and this happens, in particular, along the tunnelling trajectory). Thus it will be a sufficiently good approximation to evaluate the tunnelling probability in the, analytically much simpler, unperturbed case.

At this point, our picture of the spacetime transition will be as follows. We will take as final configurations of the tunnelling process the junctions obtained without considering the correction, which in our setup is strongly suppressed at large distances; then, the initial state, which is the $x \equiv 0$ solutions, will be "regularized" by considering the junction as the limiting case of the bounded perturbed junction when $\bar{a} \to 0$. In particular, the sign ambiguity, which affects the $x \equiv 0$ solution, will be solved by choosing the signs of the bounded trajectory of the perturbed model. These signs can be obtained in closed form consid-

ering the $x \to 0$ limit of the junction condition, which is dominated by the correction. Therefore

$$\epsilon_{\pm} = \mp 1. \quad (34)$$

Using this prescription, then, one can build the space-time diagrams representing the tunnelling process. We refer the reader to appendices for a complete discussion of the parameter space (Appendix A) and of the global spacetime diagrams representing the various physical situations (Appendix B).

To conclude the discussion, we would like to remark that, despite the fact that the regularization procedure we have described changes dramatically the situation in the region near $x = 0$ of the configuration space of the brane, the effect on the calculation we have performed is not significant. This is due to the fact that in the tunnelling region, the potential is substantially modified only in a narrow region close to the turning point corresponding to the maximum radius of the bounded solution of the modified classical junction condition. In the tunnelling region, the perturbation to the potential is finite, and by sending $\bar{a} \to 0$ the tunnelling amplitude of the modified problem is approximated arbitrarily well by our calculation in Sec. III. Of course, in the real physical problem we expect that quantum effects would prevent the brane from shrinking to zero radius: thus the mathematical limit $\bar{a} \to 0$ should be read as a more physically sound limit in which $\bar{a}$ tends to a small but finite value related to the ultimate physical nature of the brane itself (which is presently only partially understood). As a consequence, the analytical result that we have obtained (which relies on a WKB approximated description of the quantum process) can also be considered an approximation of the full quantum result at the lowest power in the ratio between the maximum radius of the bounded solution of the modified classical junction equations and x_0.

V. CONCLUSIONS

In this paper we have calculated analytically the tunnelling amplitude for a domain of spacetime of de Sitter/anti-de Sitter type in a background which, again, is de Sitter/anti-de Sitter. The analytical result holds in arbitrary spacetime dimensions greater than three, and generalizes already existing four dimensional calculations. It is not difficult to see that this result reduces, for appropriate values of the parameters, to the result found by Coleman and de Luccia [3] for the false vacuum to true vacuum transition in four spacetime dimensions. Also the results by Parke [86], again in the four dimensional case, are correctly reproduced.

We have, also, discussed extensively, in the text and in Appendix B, the spacetime structures that can arise for all possible values of the parameters characterizing the model. Some of these spacetime structures, already discussed in

the literature, are known as *tunnelling from nothing* configurations. We have also exposed a possible issue of the shell formalism in the description of the pretunnelling state and proposed a solution which relies on the above mentioned tunnelling from nothing configurations; in this way we have been able to make what we consider to be a consistent choice for the *before tunnelling* configurations. This proposal, which is implemented by considering a modification to the stress-energy tensor for the matter on the shell at small states, is motivated by the observation that if quantum effects are non-negligible on scales at which the tunnelling process occurs, they should also be non-negligible at smaller scales, where the before tunnelling configurations live. By modelling the influence of these quantum effects with a quite generic modification to the form of the stress-energy tensor at small scales, we have proposed an unambiguous rule to fix the initial configuration. This approach to the problem seems to us consistent with the level at which we are modelling quantum effects for this gravitational system, which is the *semiclassical approximation* for an *infinitesimally thin* distribution of matter and energy. At the same time, it has already been shown that, if we add a more refined matter content on the shell (as for instance a collection of gauge fields), modifications similar to the one that we have considered in this paper naturally appear [87]. Moreover, we note that it gives a very consistent picture of the tunnelling process, since all the possible types of tunnelling result in a ''sudden expansion'' of a very small region of spacetime from a small size (where quantum effects are certainly non-negligible) to a much bigger size, with radius of the order of x_0. This shows that the regularized tunnelling always models what in the literature has been called tunnelling ''from nothing.'' In our case the ''nothing'' is exactly the quantum state of the spacetime junction that we model, in an effective way, using (29). It thus seems that some tunnelling configurations present in the literature and of more difficult interpretation [67] might be ruled out by the quantum properties of matter and/or of spacetime at small scales. In fact, it is suggestive to reflect about the fact that, even in our very simplified and purely effective treatment of quantum effects before and during the tunnelling, all tunnelling processes start exactly ''from nothing'' (as interpreted above), i.e. from a configuration which is consistent with the quantum properties of the following tunnelling process.

To conclude, we would like to explicitly distinguish between the analytical result for the tunnelling probability and the proposal to interpret the *pretunnelling* configurations. Indeed the analytical result is a natural generalization of already existing calculations and it incorporates them as special cases. Its validity is completely independent from our interpretation of the before tunnelling configurations and it can represent a useful limit case to check the results of more elaborated models: for instance, a de Sitter-Schwarzschild shell configuration should reproduce,

in the limit of vanishing Schwarzschild mass, our result for a tunnelling between a de Sitter space of assigned cosmological constant and a de Sitter space with vanishing cosmological constant, i.e. Minkowski space.

ACKNOWLEDGMENTS

APPENDIX A: PARAMETER SPACE

In this appendix we will elaborate about the classification of the possible junctions between two (anti-)de Sitter spacetimes. After switching to the dimensionless formulation (see subsection II D), we remain with two parameters, i.e. $\lambda_{\pm}$, or, which is the same, α and β. We will mostly use the latter quantities in the following analysis, since many relevant features of the solutions to Israel's junction condition related to the causal structure of the full spacetime manifold $\mathcal{M}$ are easily deducible from the comparison between the two cosmological constants. In particular, in
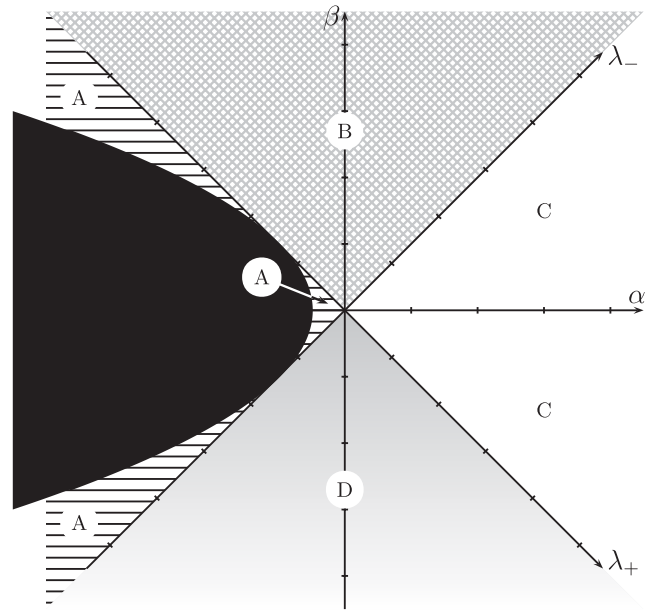

FIG. 8. The space of parameters is subdivided according to the different kinds of junctions, which can be between anti-de Sitter and anti-de Sitter spacetimes (type A), anti-de Sitter and de Sitter spacetimes (type B), de Sitter and anti-de Sitter spacetimes (type D), or de Sitter and de Sitter spacetimes (type C). The black part of the parameter space, identified by the condition $1 + 2\alpha + \beta^2 < 0$, singles out the values of the parameters for which tunnelling is not possible since the infinitely expanding solution does not exist.

Fig. 8 we give a classification of the possible solutions. The diagram shows the parameter space of the variables (α, β) *and* (λ_+, λ_-). The classification of the solutions using α and β, looks *nicely symmetric* with respect to the axis $\beta = 0$, for which $\lambda_+ = \lambda_-$; this is the primary reason why we will mostly use the (α, β) parametrization in our discussion. The (λ_+, λ_-) axes can, anyway, be conveniently used to single out the de Sitter from the anti-de Sitter spacetime. In particular, we have defined four main groups of solutions:

type A—these are solutions in which both spacetimes joined across the brane are anti-de Sitter spacetimes, i.e. we have an $\mathrm{AdS}_{(-)} - \mathrm{AdS}_{(+)}$ junction; this part of the parameter space is bounded by the parabola $\alpha = -(\beta^2 + 1)/2$ (equivalently $x_0^{-1} = 0$), whose inside is the black region where no solution exists;

type B—these solutions describe a junction of one part of de Sitter spacetime in the $\mathcal{M}_-$ manifold with a part of anti-de Sitter spacetime in the $\mathcal{M}_+$ manifold, i.e. they are $\mathrm{dS}_{(-)} - \mathrm{AdS}_{(+)}$ junctions, and play the role of counterparts of the below discussed type D solutions;

type C—these are junctions in which both spacetimes have the de Sitter geometry, i.e. we have $\mathrm{dS}_{(-)} - \mathrm{dS}_{(+)}$ junctions; in some cases, qualitatively different diagrams may arise depending on which cosmological constant is bigger, i.e. depending on the sign of β;

type D—as anticipated above, this last type of solutions is similar to the type B, with the role of "$-$" and "$+$" interchanged; we thus have $\mathrm{AdS}_{(-)} - \mathrm{dS}_{(+)}$ junctions.

The above information is not enough to completely characterize the classical spacetime obtained from the junction. In addition we need to know the behavior of the normal to the brane travelling in the spacetimes that we have determined from the diagram in Fig. 8. According to our convention the normal to the brane has its tail-tip direction going from the "$-$" to the "$+$" parts of the full spacetime $\mathcal{M}$; on the other hand in each of the two spacetimes $\mathcal{M}_\pm$ the corresponding signs $\epsilon_\pm$ determine if the normal to the brane points in the direction of increasing ($\epsilon = +1$) or decreasing ($\epsilon = -1$) radius. Using the results in (7) for $\epsilon_\pm$ we can subdivide the parameter space in three main regions, as in Fig. 9. These regions correspond to the following situations:

region 1—$\epsilon_- = \epsilon_+ = -1$, so that in both spacetimes $\mathcal{M}_\pm$ the normal $n_a|_\pm$ to the brane trajectory points in the direction of decreasing $r_\pm$;

region 2—$\epsilon_- = +1$ but $\epsilon_+ = -1$, and in $\mathcal{M}_-$ the normal to the brane trajectory $n_a|_-$ points in the direction of increasing r_- but in $\mathcal{M}_+$ the normal $n_a|_+$ to the brane trajectory points in the direction of decreasing r_+;

region 3—$\epsilon_- = \epsilon_+ = +1$; thus in both spacetimes $\mathcal{M}_\pm$ the normal $n_a|_\pm$ to the brane trajectory point in the direction of increasing $r_\pm$.

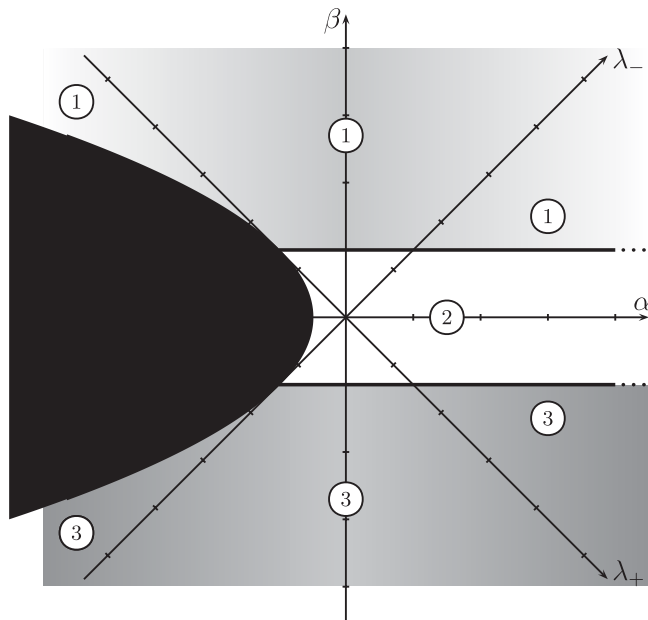FIG. 9. The parameter space can be subdivided in three other regions (strips) according to the values of the signs $\epsilon_\pm$. In region 1 we have $\epsilon_\pm = -1$, in region 2 we have $\epsilon_\pm = \mp 1$ and, finally, in region 3 we have $\epsilon_\pm = +1$.
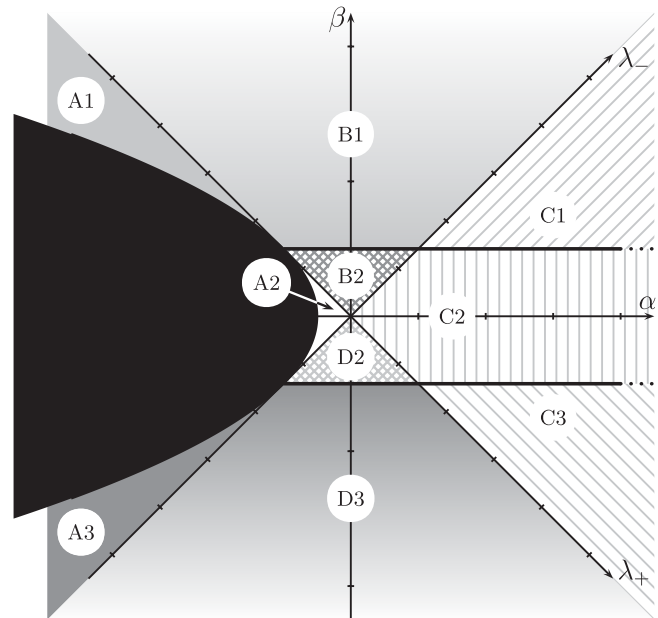

FIG. 10. In principle we have to study 10 different cases, corresponding to as many different regions in the parameter space. These regions are obtained combining the classifications in Figs. 8 and 9, so that in each region there is a well-defined type of junction with a unique choice for the signs. As we will see each of the pairs A1 and A3, B1 and D3, B2 and D2, C1 and C3 will correspond to a distinct process in spacetime; this matches well with the analytical result, in which the action turns out to be an even function of β, and gives only a total of 6 different possible processes.

We thus have various combinations of the geometries of the two spacetimes $\mathcal{M}_\pm$ according to the classification in Fig. 8; moreover we have to combine them choosing the part of spacetime on the correct side of the brane trajectory following the classification in Fig. 9. This gives a total of ten subcases, which are summarized in Fig. 10. The naming convention is the most natural, so that, for instance, the junction named B2 is a junction of type B, i.e. a $dS_{(-)}-AdS_{(+)}$ junction, with the signs as in region 2, i.e. $\epsilon_- = +1$ and $\epsilon_+ = -1$. All other names follow the same convention and we thus obtain solutions of the following types A1, A2, A3, B1, B2, C1, C2, C3, D2, D3; their causal structure is detailed in the following appendix.

APPENDIX B: PENROSE DIAGRAMS AND TUNNELLING

Here, following the classification given in the previous appendix, we show the corresponding Penrose diagrams for the classical solutions, and a pictorial representation of the corresponding tunnelling processes. For each case we give four diagrams:

(1) the complete spacetime from which we have to "cut" the $\mathcal{M}_-$ part of the bulk (with the trajectory of the bubble and the associated normal) in the top left diagram;

(2) the complete spacetime from which we have to cut the $\mathcal{M}_+$ part of the bulk (with the trajectory of the bubble and the associated normal) in the top right diagram;

(3) the junction, i.e. the full manifold $\mathcal{M}$ (again with the shell trajectory and the corresponding normal) in the bottom left diagram;

(4) a pictorial representation of the creation of the brane *via* a tunnelling process, in the bottom right diagram; in this case we have used time translation invariance to set the "tunnelling time" at the coordinate time $t = 0$ so that the top half of the diagram represents the final state (i.e. the top half of the junction in the bottom left diagram) whereas the bottom half of the diagram is a representation (detailed below) of the pretunnelling configuration.

We would like to discuss preliminarily in more detail the way in which the pretunnelling configuration is constructed. We remember that we are considering non-negligible quantum effects in the regime of the dynamics before the tunnelling. We will thus use for the signs the results coming from the modified junction (29), which are those in (34). This gives a spacetime structure consisting of two regions (which can be of the de Sitter or of the anti-de Sitter type depending on the values of α and β) both bounded by $r = 0$ and by the shell radius $r = R(\tau)$: this is the junction corresponding to the bounded solution of the modified potential (31), which is a brane starting from zero-radius and expanding to a maximum radius (much smaller than any other length scale present in the problem)

before recollapsing to $r = 0$. In the limit in which $\bar{a} \to 0$, as discussed in Sec. IV, this maximum radius tends, in fact, to zero. Nevertheless, in our representation of the spacetime before the tunnelling we have kept an arbitrarily finite size for the maximum radius, to make the diagram more readable. At the same time, we have slightly "blurred" it to make pictorially explicit that we are not dealing with a purely classical configuration but with a somehow "heuristic" representation of a spacetime where quantum effects are highly nontrivial and certainly non-negligible. We would like, anyway, to stress again that these quantum configurations will be the initial state of tunnelling processes that correspond to what in the literature has also been called "tunnelling from nothing" (see for instance [67] and references therein).

We will now present in detail the various kinds of junctions.

1. Type A

As discussed in the main text (and with reference to Fig. 10), this class of junctions consists of the matching of two anti-de Sitter spacetimes with different cosmological constants. There are three possibilities corresponding to
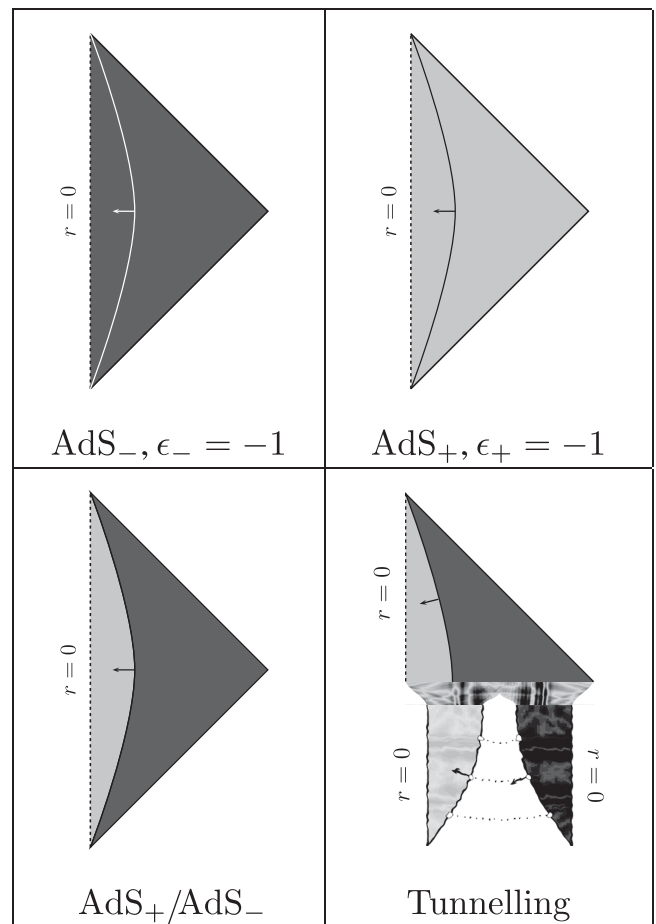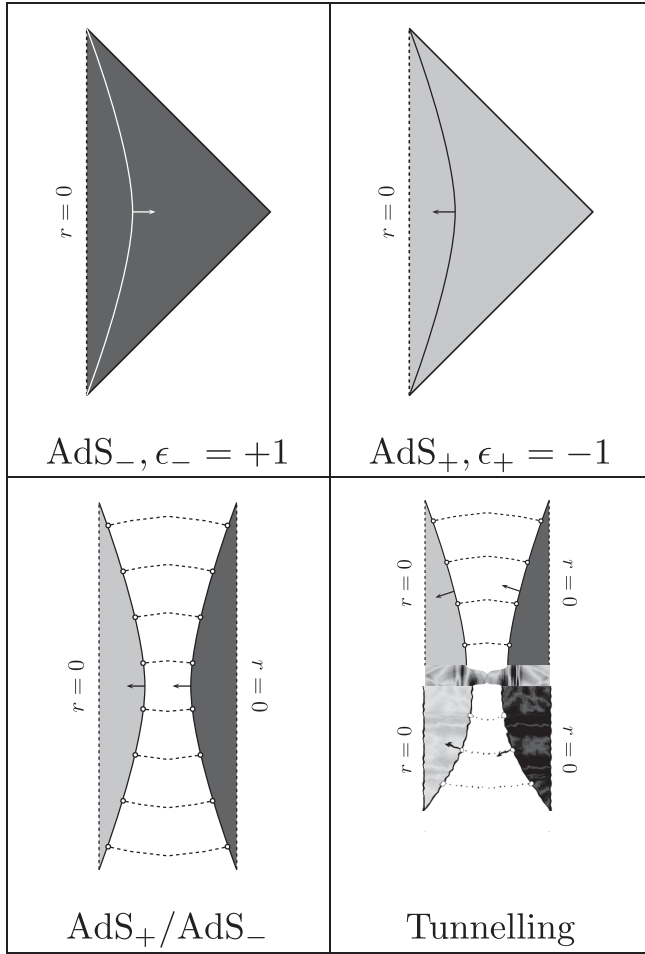

FIG. 11.   Case A1: AdS/AdS, $\epsilon_- = \epsilon_+ = -1$.

FIG. 12.   Case A2: AdS/AdS, $\epsilon_- = +1$; $\epsilon_+ = -1$.

FIG. 13.   Case A3: AdS/AdS, $\epsilon_- = \epsilon_+ = +1$.

type A1, A2, and A3 junctions, which are shown, respectively, in Figs. 11–13.

The junction of type A1 (Fig. 11) has $\epsilon_\pm = -1$, so in both anti-de Sitter spacetimes the normal to the brane points in the direction of decreasing radii. For this junction (and for all the ones in the 1 sector), $\beta > 1$, so that λ_- is always greater than λ_+. The classical junction is seen (by an observer travelling toward increasing values of the radius) as a transition from a more negative to a less negative value of the cosmological constant, when he/she crosses the brane. The global picture of the tunnelling process is then obtained according to the prescription discussed in Sec. IV. The pretunnelling spacetime has been discussed above and now consists of two "small" parts of anti-de Sitter spacetime with different cosmological constant. The tunnelling process shows the transition between a compact spacetime composed by two anti-de Sitter regions to a spacetime similar to anti-de Sitter, except for the fact that at some radius the cosmological constant changes its value.

The junction of type A2, is instead a junction where effectively a tiny junction of two anti-de Sitter spacetimes is "inflated" (Fig. 12). In this case the signs are given by
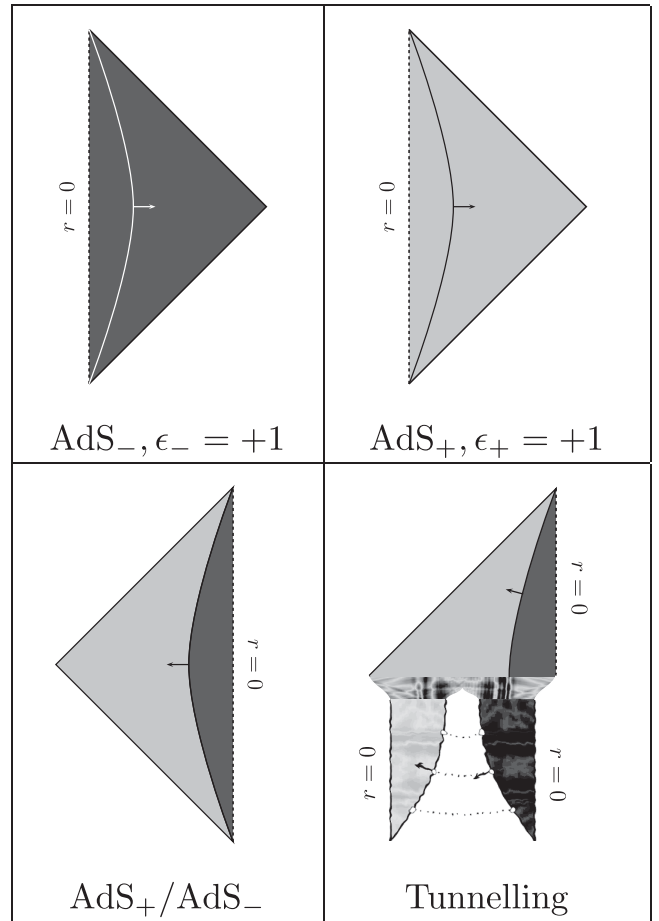
$\epsilon_\pm = \mp 1$. Thus the normal to the brane points in the direction of increasing radii in the anti-de Sitter spacetime with cosmological constant λ_-, but it points in the direction of decreasing radii in the anti-de Sitter spacetime with cosmological constant λ_+. The net effect of the tunnelling process, which starts from the already discussed initial state, is thus to inflate the pretunnelling compact spacetime into a similar, but much larger, one (note that for graphical reasons the scales in the pretunnelling and post-tunnelling parts of the diagram are different; we remember that the maximum radius of the pretunnelling state will be much smaller than any other length scale in the problem). The various diagrams are in Fig. 12.

The final type A diagram is the A3 one. This is very much as the A1 type, only that now $\epsilon_\pm = +1$; in both spacetimes the normal to the shell trajectory points in the direction of increasing radii. Thus (apparently) the role of $\mathcal{M}_\pm$ is interchanged, as shown in Fig. 13 where the dark and light gray parts look complementary to those in Fig. 11; on the other hand, now we have $\beta < -1$ so that $\lambda_+ > \lambda_-$. The global spacetime structure in the bottom left corner of Fig. 13 implies that an observer crossing the brane in the direction of increasing values of the radius, perceives again a transition from a more negative to a less

negative value of the cosmological constant. So this diagram describes exactly the same process described by type A1, as it is possible to see from the diagram in Fig. 13.

2. Type B

The type B solutions, B1 and B2, correspond to the junction of a part of a de Sitter spacetime, $\mathcal{M}_-$, with a part of anti-de Sitter spacetime, $\mathcal{M}_+$. Although the pretunnelling picture does not change very much, the configurations before the tunnelling are now de Sitter–anti-de Sitter junctions.

Let us first discuss the case B1, shown in Fig. 14. In both spacetimes, the normal to the shell points in the direction of decreasing radii, since we have $\epsilon_\pm = -1$. The $\mathcal{M}_-$ part of spacetime corresponds to the region of de Sitter complementary to the region between $r = 0$ and the brane's world volume, whereas the anti-de Sitter part $\mathcal{M}_+$ is the bounded region in the upper right picture of Fig. 14. Thus the spacetime $\mathcal{M}$ shows a transition from a negative to a positive value of the cosmological constant for an observer crossing the shell in the direction of increasing radius. The configuration before the tunnelling has been described above; the tunnelling process again "inflates" an anti-de Sitter–de Sitter junction with small volume to a much larger one, as shown in the bottom right diagram of Fig. 14.

We then come to the case B2, shown in Fig. 15. Since in this case the signs which fix the orientation of the normals are $\epsilon_\pm = \mp 1$, the situation for $\mathcal{M}_+$ is as in the previous case, but the $\mathcal{M}_-$ part of spacetime changes because of the change in the sign of ϵ_+. This gives for the junction the diagram in the bottom left part of Fig. 15. The configura-
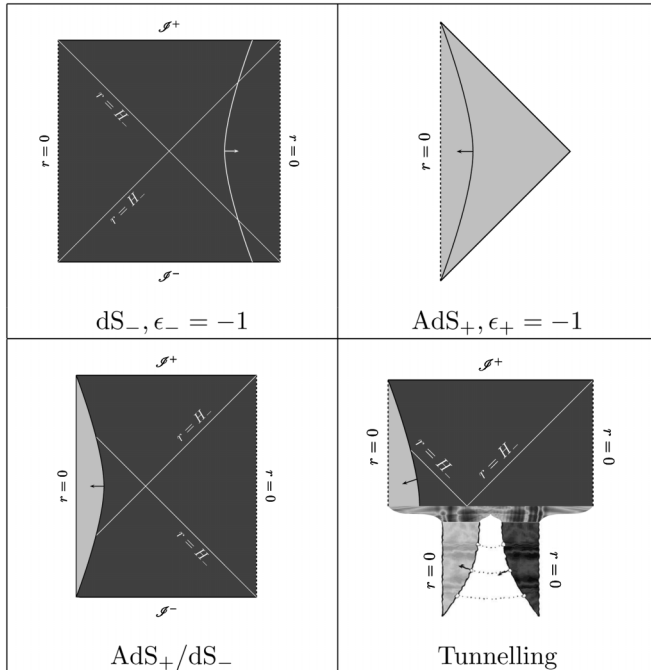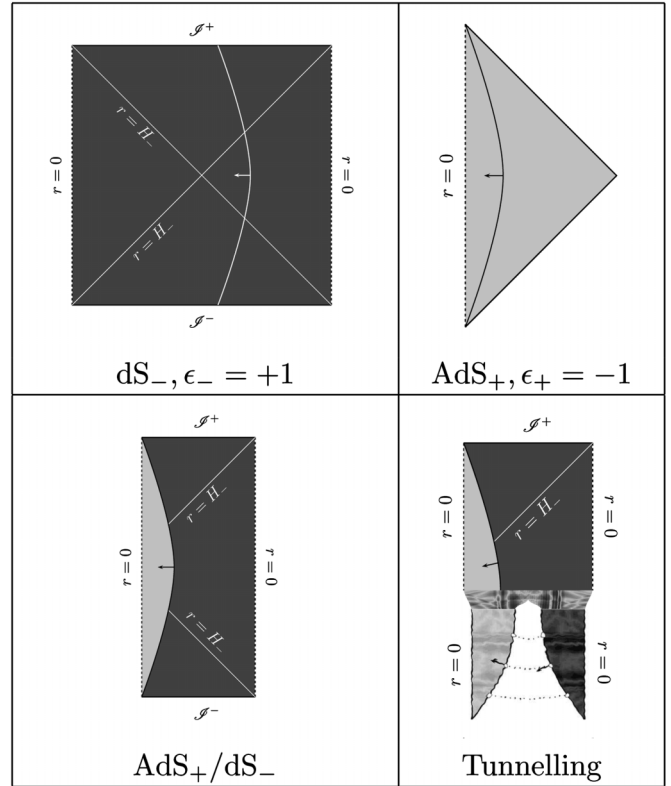

FIG. 15. Case B2: dS/AdS, $\epsilon_- = +1$; $\epsilon_+ = -1$.

tion before and after the tunnelling is shown in the bottom right corner of Fig. 15. The situation is very similar to the one in the previous case.

3. Type C

Type C solutions are the "de Sitter counterpart" of the type A solution. The main difference (not related to the spacetime structure) is that whereas for anti-de Sitter junctions the values of the cosmological constant are restricted (i.e. given two arbitrary values a junction might not exist) de Sitter junctions exists for all values of the cosmological constants $\lambda_\pm$ (this is clear from Fig. 10). Please, also remember that now the pretunnelling diagram will consist of a junction of two de Sitter spacetimes with different cosmological constants and with all the other properties described above.

Let us start with case C1, shown in Fig. 16. For this junction, the signs are $\epsilon_\pm = -1$, so in both de Sitter spacetimes the normals to the brane point in the direction of decreasing radii. Moreover, since in this case $\beta > 1$, the cosmological constant in $\mathcal{M}_-$ will be bigger than the cosmological constant in $\mathcal{M}_+$, so that the cosmological horizon H_- will be smaller than H_+. The diagram for the junction is shown in the bottom left part of Fig. 16. It is interesting to see some effects of the brane on the spacetime structure. There are observers that crossing the brane can move behind the cosmological horizon of $\mathcal{M}_-$ without going through H_-. They can also come out, by crossing the
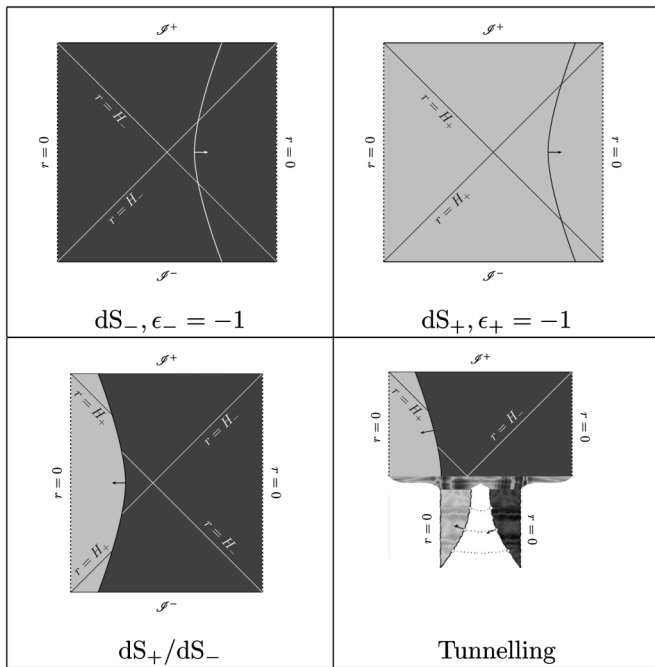

FIG. 14. Case B1: dS/AdS, $\epsilon_- = \epsilon_+ = -1$.

FIG. 16. Case C1: dS/dS, $\epsilon_- = \epsilon_+ = -1$.

FIG. 17. Case C2: dS/dS, $\epsilon_- = +1$; $\epsilon_+ = -1$.

brane in the opposite direction. At the same time observers, by moving accurately and with proper timing, might end up behind the cosmological horizon of $\mathcal{M}_+$ without crossing any horizon but using the shell as a "gate."[11] As usual no additional considerations are required for the before tunnelling configuration. We note, instead, that the semiclassical transition has again the effect of "inflating" a small quantum spacetime region, as clearly shown in Fig. 16.

We now discuss case C2, in which the signs are $\epsilon_\pm = \mp 1$. Then the normal to the brane in the de Sitter space with cosmological constant λ_- points in the direction of increasing radii, whereas the normal to the brane in the de Sitter space with cosmological constant λ_+ points in the direction of decreasing radii. We have again two regions of spacetime of the de Sitter type but with a different cosmological constant joined across the brane (bottom right part of Fig. 17). The full picture of the tunnelling process requires the consideration of the same initial configuration used in case C1 above. We also point out that in this case, the sign of β is not fixed, so either of the cosmological constants $\lambda_\pm$ may be the bigger. In particular, the junction in the bottom left corner of Fig. 17 shows the situation in which $\lambda_+ < \lambda_-$, so that $H_+ > H_-$. In the bottom right part of Fig. 17 a representation of the tunnelling process is shown.

The last junction of the C type is C3, for which the usual set of diagrams is shown in Fig. 18. As all C type ones, this

is a junction between two de Sitter spacetimes and since $\beta < -1$ the relation between the cosmological constants is $\lambda_+ > \lambda_-$, so that $H_+ < H_-$. At this stage we might wonder if this junction is the same as C1 (mirroring what happens between the junctions of the A1 and A3 type). We will see that this is indeed the case. The normals now point in both spacetimes toward the direction of increasing radii (since $\epsilon_\pm = +1$). Thus the junction is as in the bottom left part of Fig. 18. When we consider also the

FIG. 18. Case C3: dS/dS, $\epsilon_- = \epsilon_+ = +1$.

<hr>

[11]These considerations might be modified if we consider the influence of the observer on spacetime. To neglect this influence, as a first approximation, is fairly common in the literature to obtain some hints about the global spacetime structure.
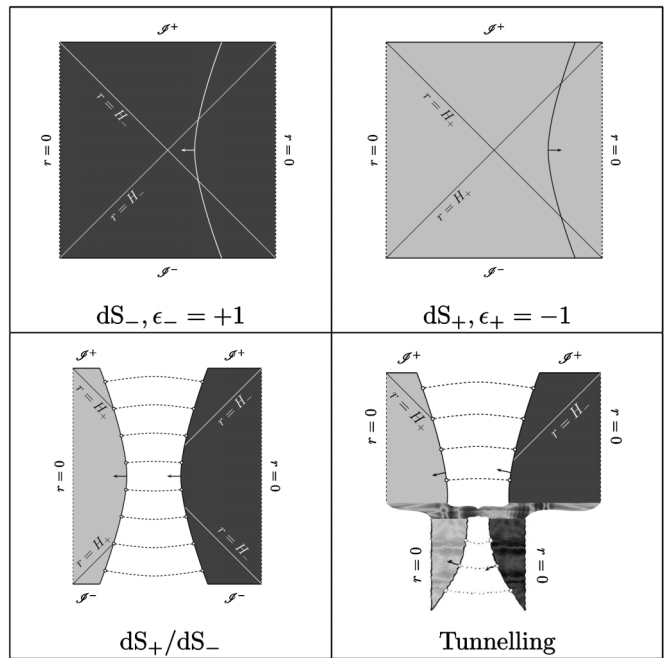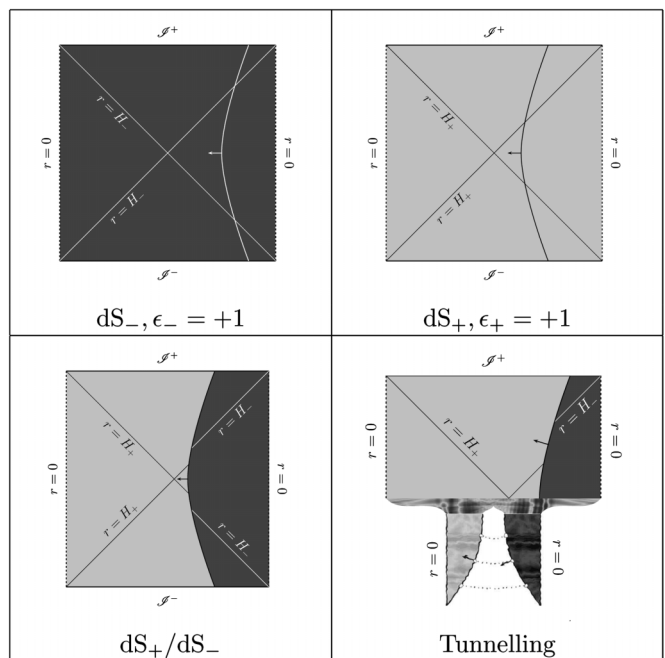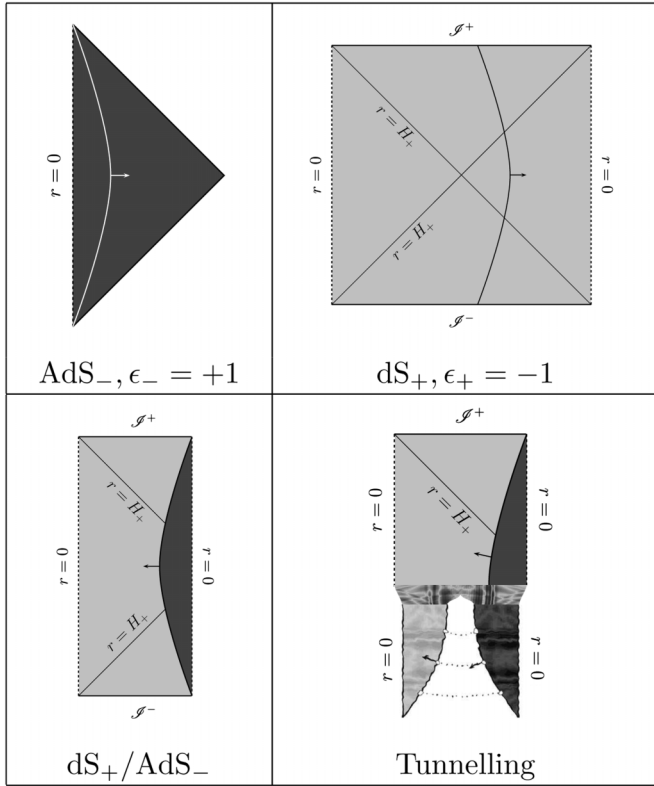
FIG. 19.   Case D2: AdS/dS, $\epsilon_- = +1$; $\epsilon_+ = -1$.

FIG. 20.   Case D3: AdS/dS, $\epsilon_- = \epsilon_+ = +1$.

configuration before tunnelling, we see that the diagram in the bottom right part of Fig. 16 is the "switched color and reflected" version of the one in the bottom right part of Fig. 18: we remember now that in the C1 case λ_- in the light gray part was bigger than λ_+ in the dark side, but now exactly the opposite happens. Thus, despite the different coloring, case C3 represents the same physical situation of case C1. This observation makes it interesting to complete the analysis for the remaining two cases, which is done in the following subsection.

4. Type D

To conclude the analysis of the global spacetime structure we have to analyze what happens for the last kind of junctions, those of type D. These are junctions between de Sitter and anti-de Sitter spacetimes, so that the pretunnelling configuration will also change accordingly, as we have discussed for the previous cases.

The case of the junction of type D2 is characterized by the following signs: $\epsilon_\pm = \mp 1$. This means that in the anti-de Sitter side the normal points in the direction of increasing radii, whereas in the de Sitter part, it points in the direction of decreasing radii. Thus the junction, shown in the bottom left corner of Fig. 19, is the mirror image of the B2 case. Again, the considerations in Sec. IV determine the geometry before the tunnelling. This brings, in complete analogy with the B2 case, to the picture of the tunnelling process given in the bottom right part of Fig. 19; again,
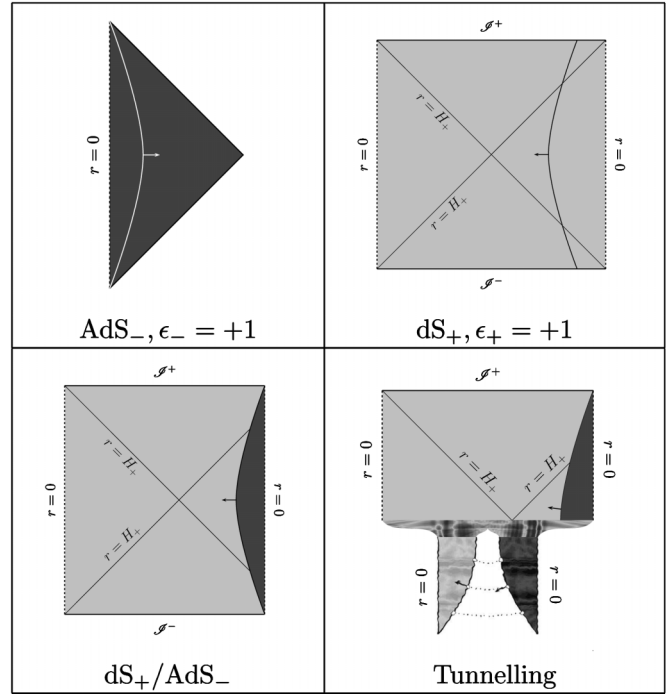
apart from the different colors, this case is the same as B2 also in connection with the semiclassical tunnelling process.

We have thus only one case left, which is quickly dealt with, namely, D3. It is now not difficult to anticipate that this process will turn out to be identical to B1, that appears in Fig. 14. Indeed the signs are now $\epsilon_\pm = +1$, so that in both spacetime the normals point in the direction of increasing radii. By the usual procedure we are thus led to the spacetime diagram shown in the bottom left part of Fig. 20. Part of this diagram will constitute the final state of the tunnelling process. The initial state is obtained as usual and the picture of the tunnelling process is as in the bottom right part of Fig. 20.

5. Comments

From the analysis developed so far we have seen that, although in principle we have ten different tunnelling processes, in fact process A1 is the same as A3, process B1 is the same as D3, process B2 is the same as D2, and process C1 is the same as C3. We are thus left with only six distinct processes. From "symmetry considerations," it is natural to notice that $|\beta|$, not β itself, is the relevant quantity (together with α) to classify the possible tunnelling configurations. We will thus not be surprised if the tunnelling amplitude will be a function of $|\beta|$, or, which is the same, an *even function of β*. We would also like to note already here that all the tunnelling processes can be interpreted as a very large expansion of a small *quantum* region of spacetime.

[1] S. Coleman, Phys. Rev. D **15**, 2929 (1977); **16**, 1248(E) (1977).

[2] J. C. G. Callan and S. Coleman, Phys. Rev. D **16**, 1762 (1977).

[3] S. Coleman and F. D. Luccia, Phys. Rev. D **21**, 3305 (1980).

[4] K. Lee and E. J. Weinberg, Phys. Rev. D **36**, 1088 (1987).

[5] S. W. Hawking, I. G. Moss, and J. M. Stewart, Phys. Rev. D **26**, 2681 (1982).

[6] W. Z. Chao, Phys. Rev. D **28**, 1898 (1983).

[7] K. Sato, M. Sasaki, H. Kodama, and K.-I. Maeda, Prog. Theor. Phys. **65**, 1443 (1981).

[8] H. Kodama, M. Sasaki, K. Sato, and K.-I. Maeda, Prog. Theor. Phys. **66**, 2052 (1981).

[9] K. Sato, Prog. Theor. Phys. **66**, 2287 (1981).

[10] K.-I. Maeda, K. Sato, M. Sasaki, and H. Kodama, Phys. Lett. B **108**, 98 (1982).

[11] K. Sato, H. Kodama, M. Sasaki, and K.-I. Maeda, Phys. Lett. B **108**, 103 (1982).

[12] H. Kodama, M. Sasaki, and K. Sato, Prog. Theor. Phys. **68**, 1979 (1982).

[13] V. A. Berezin, V. A. Kuzmin, and I. I. Tkachev, Phys. Rev. D **36**, 2919 (1987).

[14] S. K. Blau, E. I. Guendelman, and A. H. Guth, Phys. Rev. D **35**, 1747 (1987).

[15] A. Aurilia, R. S. Kissack, R. Mann, and E. Spallucci, Phys. Rev. D **35**, 2961 (1987).

[16] E. Farhi, A. H. Guth, and J. Guven, Nucl. Phys. **B339**, 417 (1990).

[17] V. A. Berezin, V. A. Kuzmin, and I. I. Tkachev, Phys. Rev. D **43**, R3112 (1991).

[18] M. Sasaki, T. Tanaka, K. Yamamoto, and J. Yokoyama, Phys. Lett. B **317**, 510 (1993).

[19] T. Tanaka, Nucl. Phys. **B556**, 373 (1999).

[20] A. Khvedelidze, G. V. Lavrelashvili, and T. Tanaka, Phys. Rev. D **62**, 083501 (2000).

[21] A. Vilenkin, Phys. Rev. D **27**, 2848 (1983).

[22] A. D. Linde, Lett. Nuovo Cimento **39**, 401 (1984).

[23] A. D. Linde, Zh. Eksp. Teor. Fiz. **87**, 369 (1984) [Sov. Phys. JETP **60**, 211 (1984)].

[24] D. Stojkovic, G. D. Starkman, and R. Matsuo, arXiv:hep-ph/0703246.

[25] K. V. Kuchar and M. P. J. Ryan, Phys. Rev. D **40**, 3982 (1989).

[26] G. W. Gibbons and S. W. Hawking, Phys. Rev. D **15**, 2738 (1977).

[27] R. Bousso and S. W. Hawking, Phys. Rev. D **52**, 5659 (1995).

[28] R. Bousso and S. W. Hawking, Phys. Rev. D **54**, 6312 (1996).

[29] R. R. Caldwell, H. A. Chamblin, and G. W. Gibbons, Phys. Rev. D **53**, 7103 (1996).

[30] T. Vachaspati and M. Trodden, Phys. Rev. D **61**, 023502 (1999).

[31] J. Gariel and G. L. Denmat, Classical Quantum Gravity **16**, 149 (1999).

[32] P. Wang and X.-H. Meng, Classical Quantum Gravity **22**, 283 (2005).

[33] A. Aguirre and M. C. Johnson, Phys. Rev. D **72**, 103525 (2005).

[34] S. W. Hawking, Phys. Rev. D **18**, 1747 (1978).

[35] J. B. Hartle and S. W. Hawking, Phys. Rev. D **28**, 2960 (1983).

[36] A. Vilenkin, Phys. Rev. D **30**, 509 (1984).

[37] S. Carlip, Phys. Rev. D **46**, 4387 (1992).

[38] A. Vilenkin, Phys. Rev. D **58**, 067301 (1998).

[39] R. Bousso and A. Chamblin, Phys. Rev. D **59**, 084004 (1999).

[40] G. W. Gibbons, Classical Quantum Gravity **15**, 2605 (1998).

[41] A. Vilenkin, Phys. Lett. B **117**, 25 (1982).

[42] W. Fischler, D. Morgan, and J. Polchinski, Phys. Rev. D **41**, 2638 (1990).

[43] W. Fischler, D. Morgan, and J. Polchinski, Phys. Rev. D **42**, 4042 (1990).

[44] J. Garriga, Phys. Rev. D **49**, 6327 (1994).

[45] B. Freivogel, V. E. Hubeny, A. Maloney, R. C. Myers, M. Rangamani, and S. Shenker, J. High Energy Phys. 03 (2006) 007.

[46] L. Anchordoqui, C. Nunez, and K. Olsen, J. High Energy Phys. 10 (2000) 50.

[47] S. Kar, J. High Energy Phys. 10 (2006) 052.

[48] S. Kar, Phys. Rev. D **74**, 126002 (2006).

[49] S. J. Kolitch and D. M. Eardley, Phys. Rev. D **56**, 4651 (1997).

[50] S. J. Kolitch and D. M. Eardley, Phys. Rev. D **56**, 4663 (1997).

[51] Y. Nutku, M. B. Sheftel, and A. A. Malykh, Classical Quantum Gravity **14**, L59 (1997).

[52] A. Aurilia, H. Nicolai, and P. K. Townsend, Nucl. Phys. **B176**, 509 (1980).

[53] M. Henneaux and C. Teitelboim, Phys. Lett. B **143**, 415 (1984).

[54] A. Aurilia, G. Denardo, F. Legovini, and E. Spallucci, Phys. Lett. B **147**, 258 (1984).

[55] A. Aurilia, G. Denardo, F. Legovini, and E. Spallucci, Nucl. Phys. **B252**, 523 (1985).

[56] J. D. Brown and C. Teitelboim, Phys. Lett. B **195**, 177 (1987).

[57] J. D. Brown and C. Teitelboim, Nucl. Phys. **B297**, 787 (1988).

[58] F. Mellor and I. Moss, Classical Quantum Gravity **6**, 1379 (1989).

[59] J. L. Feng, J. March-Russel, S. Sethi, and F. Wilczek, Nucl. Phys. **B602**, 307 (2001).

[60] S. Ansoldi, A. Aurilia, and E. Spallucci, Phys. Rev. D **64**, 025008 (2001).

[61] A. Gomberoff, M. Henneaux, C. Teitelboim, and F. Wilczek, Phys. Rev. D **69**, 083520 (2004).

[62] J. Garriga and A. Megevand, Int. J. Theor. Phys. **43**, 883 (2004).

[63] C. Barrabes and W. Israel, Phys. Rev. D **43**, 1129 (1991).

[64] W. Israel, Nuovo Cimento B **44**, 1 (1966); **48**, 463(E) (1967).

[65] R. Geroch and J. Traschen, Phys. Rev. D **36**, 1017 (1987).

[66] R. Maartens, Living Rev. Relativity **7**, 7 (2004), http://www.livingreviews.org/lrr-2004-7.

[67] S. Ansoldi, A. Aurilia, R. Balbinot, and E. Spallucci, Classical Quantum Gravity **14**, 2727 (1997).

[68] P. Hajicek and J. Bicak, Phys. Rev. D **56**, 4706 (1997).

[69] J. L. Friedman, J. Louko, and S. N. Winters-Hilt, Phys. Rev. D **56**, 7674 (1997).

[70] P. Hajicek and J. Kijowski, Phys. Rev. D **57**, 914 (1998).

[71] P. Hajicek, Phys. Rev. D **57**, 936 (1998).

[72] J. L. Friedman, J. Louko, and B. F. Whiting, Phys. Rev. D **57**, 2279 (1998).

[73] P. Hajicek, Phys. Rev. D **58**, 084005 (1998).

[74] P. Hajicek and J. Kijowski, Phys. Rev. D **61**, 129901(E) (2000).

[75] S. Mukohyama, Phys. Rev. D **65**, 024028 (2001).

[76] R. Capovilla, J. Guven, and E. Rojas, Classical Quantum Gravity **21**, 5563 (2004).

[77] C. Barrabes and W. Israel, Phys. Rev. D **71**, 064008 (2005).

[78] G. L. Alberghi, R. Casadio, and G. Venturi, Phys. Rev. D **60**, 124018 (1999).

[79] G. W. Gibbons and S. W. Hawking, Phys. Rev. D **15**, 2752 (1977).

[80] Misner, Thorne, and Wheeler, *Gravitation* (Freeman, San Francisco, 1973).

[81] V. I. Arnold, *Mathematical Methods of Classical Mechanics* (Springer-Verlag, Berlin, 1978).

[82] A. Aurilia, M. Palmer, and E. Spallucci, Phys. Rev. D **40**, 2511 (1989).

[83] S. Ansoldi and L. Sindoni, in *Proceedings of the 6th International Symposium on Frontiers of Fundamental Physics (FFFP6), Udine, Italy, 2004* (Frontíeres, Gif sur Yvette, France, 2004), p. 69.

[84] S. Ansoldi, in *Proceedings of the 16th Workshop on General Relativity and Gravitation (JGRG16), Niigata, Japan, 2006*, edited by K.-I. Oohara, T. Shiromizu, K.-I. Maeda, and M. Sasaki (JGRG16 Organizing Committee, Kyoto, 2007).

[85] S. Ansoldi, Proceedings of ''From Quantum to Emergent Gravity: Theory and Phenomenology'', SISSA, Trieste, Italy, 2007 [Proc. Sci. (to be published)].

[86] S. Parke, Phys. Lett. B **121**, 313 (1983).

[87] E. I. Guendelman and J. Portnoy, Classical Quantum Gravity **16**, 3315 (1999).